Wissenschaftliche Arbeit zur Erlangung des Grades eines
Bachelor of Science

im Studiengang Medizintechnik

an der

Hochschule Bremerhaven

zusammen mit

Alfred-Wegener-Institut für Polar- und Meeresforschung
Sektion Integrative Ökophysiologie
in Bremerhaven

The Kraken Pulse Oximeter

Developing a concept to non-invasively measure blood oxygen saturation in Cephalopods.

vorgelegt am 28.04.2022 von

Bagavi Elancheliyan (35802)

Referent:
Prof. Olaf Eick
Hochschule Bremerhaven, Bremerhaven

Korreferent:
Dr. Felix C. Mark
Alfred-Wegener-Institut für Polar- und Meeresforschung, Bremerhaven

Acknowledgment

I have received a great deal of support and encouragement while writing this thesis.

Firstly, I would like to thank Dr. Felix C. Mark for supervising my work. Your insightful questions and feedback helped sharpen my thinking and complete the thesis.

I want to thank Prof. Dr. Olaf Eick for taking the responsibility of the first examiner.

I wish to show my appreciation to Janakan Kathirkamanathan and Abirami Puvanendran for assisting me with their professional expertise.

Completing this thesis would not have been possible without my family and friends. Your assistance, motivation, and effort to provide me with distractions outside of the research are highly appreciated.

Finally, I would like to thank the following people for their support: Laavanya Naguleswaran, Akshaya Pathmanathan, Ahrabi Logachandran and Hannes Bente.

Abstract

As part of an international project to bring humane slaughtering methods to cephalopod molluscs, the Alfred-Wegener-Institute in Bremerhaven contributes by facilitating a subproject. The overall aim of the international project is to prevent marine animals from experiencing pain and distress during slaughter by improving on current methods.

The subproject aims to conceive a proof of concept based on pulse oximetry to measure oxygen saturation in cephalopod molluscs. The created system ought to be the base for prospective hardware to analyse cephalopods during anaesthetized conditions to establish enhanced humane stunning procedures. The creation of a transmissive-based pulse oximeter prototype using Arduino, a physical computing platform, represents a pivotal phase within the scope of this thesis. Furthermore, this thesis deals with the development of a customised calibration method to calculate SpO_2 values, an alternative to the previously applied software, that yielded erroneous results. The required data to perform customised calculations were collected from measurements done on test subjects. Finally, the conception of a model for cephalopods is presented based on the outcomes of the prototype. Despite difficulties due to the inconvenient structure of the hardware, general proof of concept for the developed prototype can be declared at the end of the project.

Based on these findings the realization of a suitable concept for cephalopods is presumably feasible. This paper is intended to act as a foundation for further advancements toward the non-invasive measurement of oxygen saturation in cephalopods through the application of the theoretical and practical knowledge that was acquired throughout this project.

Table of Contents

List of Figures

List of Tables

List of Equations

Abbreviations

AC	Alternating current
avBPM	Average beats per minute
AWI	Alfred-Wegener-Institute
CephRes	Association for Cephalopod Research
GND	Ground
COHb	Carboxyhemoglobin
CO_2	Carbon dioxide
DC	Direct current
Fe	Iron
Hb	Hemoglobin
Hc	Hemocyanin
HSA	Humane Slaughter Association
IDE	Integrated development platform
IR	Infrared
λ	Lambda
LED	Light-emitting diode
mA	Milliampere
MetHb	Methemoglobin
mL	Millilitre
NIR	Near-infrared
Nm	Nanometre
O_2Hb	Oxygenated hemoglobin
O_2	Oxygen
PPG	Photoplethysmography
R	Ratio
SaO_2	Arterial oxygen saturation
SpO_2	Peripheral oxygen saturation
UV	Ultraviolet
V	Voltage
VIS	Visible light

1. Introduction

Pulse oximetry can be categorized as one of the most advanced applications for non-invasive patient monitoring since achieving relevance in the medical field in the early 1980s (Wabnitz & Klein, 1999). It has become a tool of a standard of care in medicine, frequently being applied intraoperatively in adults and the neonatal intensive care (Bowes 3rd, et al., 1989). By utilising pulse oximetry, physicians are able to measure oxygen concentration in the patient's blood. The peripheral oxygen saturation level is referred to as SpO_2, as it is measured at the peripherals of the body. It is regarded as the fifth vital parameter besides pulse rate, body temperature, blood pressure, and respiration rate (Peterson, 2007).

Similarly, observing oxygen levels in animals can be helpful in determining their health condition. Current stunning methods for marine animals such as cephalopods molluscs (i.e., cuttlefish, squid, and octopus) are considered inhumane. Thus, several European institutions are collaborating on an international project to improve the welfare of cephalopod molluscs. The implementation of pulse oximetry for the purpose of assessing the condition of the animals during anaesthesia and the preparation for slaughter is promising. As a contribution to this project, the goal of this thesis is to develop a concept to measure blood oxygen saturation in cephalopods.

This thesis comprises of an overview of the theoretical foundation followed by the project's gradual implementation of the prototype pulse oximeter, beginning with an elaboration of the research design in section 3. It includes the methodical approach to assembly, data processing, and analysis. Results are presented in section 4 and discussed extensively in the following segment. Ultimately, the work is rounded off with a conclusion.

1.1 Humane Slaughter Association

One of many institutions of the international project is the British Humane Slaughter Association. It is an independent charity organization founded in 1911, which highlights and promotes the importance of the welfare of animals intended for human consumption through the process of fishing, marketing, transport, and slaughter. They use scientific, technical, and educational advances to emphasize current inhumane slaughter practices requiring refinement. The HSA is internationally known for solutions to improve food welfare by taking the initiative to

research the manner of slaughtering and handling of farmed species (Association, 2022).

1.2 Bringing humane slaughtering to cephalopod molluscs with the Association for Cephalopod Research

The HSA is funding an international project titled “Bringing Humane Slaughtering to cephalopod molluscs: an integrative approach.” The project is coordinated by the Italian-based non-profit Association of Cephalopod Research, collaborating with other European research institutions. CephRes was established in 2011 and promotes scientific knowledge about cephalopods. This joint project focuses on the scientific research and development of procedures to identify humane approaches for stunning cephalopod molluscs. To analyse the different physiological states of marine animals in the process of slaughter, the researchers utilise methodologies rooted in neurophysiology, physiology, molecular biology, and behaviour. Ultimately, the primary objective of this collaboration is to improve animal welfare and develop humane methods for killing cephalopod molluscs that take the pain, suffering, and distress of the animals into account (CephRes, 2022).

1.3 The Alfred-Wegener-Institute for Polar- and Marine Research

Established in 1980, the Alfred-Wegener-Institute is a research facility for polar and marine research with locations based throughout Germany: Bremerhaven, Helgoland, Oldenburg, Sylt, and Potsdam. The institute is named after the geoscientist and polar researcher Alfred Wegener, known for developing the theory of continental drift (Salewski, 2022). AWI is one of few facilities worldwide conducting scientific research in the Arctic and Antarctic, the North Sea, and the coastal regions of Germany. At present, several scientific research projects at AWI are undertaken regarding climate change to assess the impact on living beings, their habitat, and the ecosystem of these polar regions (Alfred-Wegener-Institut, 2021). A sub-project conducted as part of the international project mentioned above is carried out within the integrative ecophysiology section located at AWI’s headquarters in Bremerhaven, Germany. The aim of this sub-project, which is the subject for this thesis, is to develop a concept to measure blood oxygen saturation on resting, anaesthetized cephalopods non-invasively. This collaboration aims to

ultimately create a custom-built pulse oximeter with which the blood oxygen saturation in cephalopods can be measured.

1.4 Project description

The identified research gap defines the unconventional thesis design outlined in this thesis. In the scope of this thesis, the main ambition is to construct a custom-built prototype identical to a commercially available pulse oximeter and achieve a proof of concept. The medical field of pulse oximetry will provide the basis for the conception of this project as the core functionality of commercially available pulse oximeters can be transferred to be applied accordingly. By combining this with the open-source development platform Arduino, the purpose is to conceptualize a device applicable to cephalopods and provide the central capabilities of a pulse oximeter. However, due to different oxygen-binding molecules in the blood, hemocyanin for cephalopods, and hemoglobin for humans, certain technicalities in hardware and software need to be adjusted accordingly. The structure of this project consists of multiple steps. After assembling a transmissive-based hardware using suitable electronic components, the results will be analysed. The final step will be examining the possibility of adapting the system to the physiology of cephalopods. At the end of this, there will be an assessment of practicability to deduce a proof of concept. Subsequently, the aim is to create a concept for a prototype for cephalopods based on previously gathered results.

2. Theoretical Framework

The following section will provide a theoretical baseline to establish the fundamental concept of this project through a comprehensive review of the foundational literature.

2.1 Physiological Background

Blood and its specific components play a pivotal role to the foundation of this thesis and will be elaborated in this subsection.

The average amount of blood in a normal adult is approximately 4-6 litres. This makes up 6-8% of the body's weight. Blood is a fluid connective tissue pivotal to the human body combining various elements of complex structures. It is composed of red blood cells (erythrocytes), white blood cells (leukocytes), platelets (thrombocytes), and a solution of extracellular matrix referred to as the plasma, binding all constituent parts together (Brandes, et al., 2019). The plasma represents approximately 55% of the blood volume while blood cells make up 45% (Schaller, et al., 2008). Blood's primary responsibilities lie in the transportation of respiratory gases, dispensing essential nutrients, and the detoxification of cells to keep the milieu of the blood at a constant. In addition, it acts as a defence mechanism against invading pathogens and blood loss by initiating haemostasis and for moving hormones and heat (Schneider & Rein, 1971).

Leucocytes represent three percent of blood cells with a concentration of $7x10^9$ cells/litre. The white blood cells work for the body's immune defence and are distinguished into cell-creating antibodies and memory cells (Schaller, et al., 2008). Memory cells' ability to recall foreign particles previously exposed to allows for a faster and stronger response and enhances immunity against reencountering pathogens. Thrombocytes are represented at a concentration of $250x10^9$ cells/litre and are significant for compressing injured vessels and facilitating the thrombus formation (Brandes, et al., 2019).

96% of all blood cells are small flexible biconcave, flattened erythrocytes with a concentration of $5x10^{12}$ cells/litre (Brandes, et al., 2019). Erythrocytes' flexibility is facilitated by their thin membrane container structure filled with liquid enabling easy passage through the narrow blood capillary system. The flat shape of erythrocytes provides a large surface, allowing a straightforward diffusion process since the outlet area for molecules is more extensive, and the distance is shorter (Brandes, et al.,

2019). The prime function of erythrocytes is to transport oxygen from the lungs to peripheral tissues and carry the by-product carbon dioxide back to the lungs for expiration. The transportation is enabled by red blood cells' primary protein, hemoglobin. Each red blood cell carries roughly $3x10^8$ hemoglobin molecules (Schaller, et al., 2008).

2.1.1 Characteristics of hemoglobin

Hemoglobin is a respiratory pigment present in almost all vertebrates except arctic fish and some invertebrates. As illustrated in Figure 1a, hemoglobin is a tetrameric globular protein comprised of two α and two β polypeptide chains of linear sequences of amino acids (Webster, 1997).

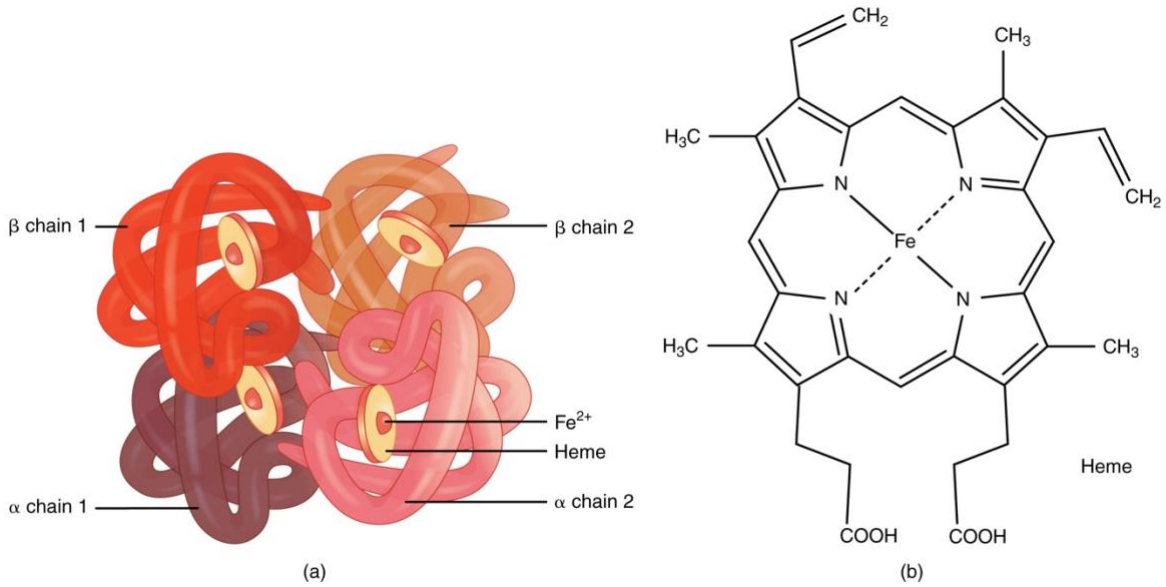

Figure 1: Hemoglobin structure.
Source: (OpenStax, 2013)

Each polypeptide chain, or globin chain, harbours one prosthetic group fixed at a particular position (see Fig. 1a). This prosthetic group is called the heme, which gives blood its characteristically red colour. The heme consists of an iron atom (Fe) at the centre of a porphyrin ring (see Fig. 1b) (Perutz, 1978). One polypeptide chain and its heme group make one hemoglobin subunit. A single oxygen molecule can bind reversibly with one iron atom present in the heme (Koecke, 1975). As a result, every hemoglobin subunit can take on four oxygen molecules. However, oxygen has a low solubility for which only 3mL of absorbed oxygen molecules are dissolved into the plasma, while 98% bind to the protein. The oxygen-binding capacity for one gram of Hb is around 1.34mL O_2 (Perutz, 1978). With the help of oxygen-binding

Hb, the body can distribute 65 times more oxygen for the same amount of plasma than without (Webster, 1997). Apart from oxygenated Hb and deoxygenated Hb, Hb is present in two additional derivatives: methemoglobin and carboxyhemoglobin (Wabnitz & Klein, 1999). COHb are molecules binding carbon monoxide instead of oxygen, due to which the oxygen-binding is prevented for these subunits. They make up around two percent of Hb molecules (Wabnitz & Klein, 1999). MetHb concentration amounts to approximately one percent but arises when exposed to diverse chemical reactions. Similarly, MetHb is prevented from transporting because of its chemical compound (Webster, 1997). The following paragraph describes the process of oxygen distribution in the body.

2.1.2 Oxygen transport

Adequate oxygen distribution within the body is indispensable for humans. Decreasing oxygenation levels in the body can lead to the rapid deterioration of tissue and hence bring life-threatening circumstances. The oxygenation of the body can be divided into two stages: first pulmonary and, subsequently, systemic circulation (Bright, 2018). The two essential functions of these systems are to provide each cell in the human body with oxygen inhaled from the environment and transport metabolically produced by-products of respiration such as carbon dioxide back to the lungs for exhalation. Blood is pumped by the heart through the aorta and circulates the body through its arteries, veins, and capillaries (Bright, 2018). Pulmonary circulation is responsible for circulating blood between the lungs and heart for gas exchange. During this distribution, air inhaled from the environment enters the lungs, where oxygen molecules bind to hemoglobin molecules of the red blood cells. Afterward, blood flows to the heart. The blood distribution from the heart to the rest of the body is systemic circulation. It is responsible for carrying oxygenated blood to the narrow capillary beds to diffuse into the cells. After hemoglobin releases the oxygen molecules, it absorbs the carbon dioxide. Subsequently, it is transported back to the heart. An erythrocyte's easily deformable structure is ideal for passing through the constricted capillaries, where the red blood cells release oxygen. Released, the oxygen molecules diffuse into the body tissues through the capillary walls (Brandes, et al., 2019).

The pulsatile blood flow in the artery allows for the determination of physiological condition known as the pulse. Pulse is a rhythmic change in the artery's diameter

caused by the contraction mechanism of the heart. The periodical blood volume change is differentiated between systole, the heart's contractions causing a pulsatile blood flow in the artery, and diastole. The ensuing relaxation period of the heart is referred to as the diastole. The pulse is the number of heartbeats within a minute. The heartbeats can be felt in places on the body where an artery is close to the skin. The resting heart rate in healthy adults is between 60 and 100 beats per minute (Webster, 1997).

2.2 Principles of Pulse Oximetry

This section provides a review of the fundamentals of pulse oximetry and the essential components a pulse oximeter is comprised of. Due to the depth this topic presents, this section acknowledges the basic outline of pulse oximetry.

Oxygen saturation (SaO_2) is the ratio of the concentration of oxygenated hemoglobin compared to the concentration of total hemoglobin present in arterial blood (Alian & Shelley, 2022).

Oximetry is the general terminology used to describe the optical measurement of oxygenated Hb in the blood. Pulse oximetry is one of the various methodologies utilised to estimate oxygen levels (Webster, 1997).

Pulse oximetry is a non-invasive physiologic monitoring device used in medicine and veterinary science to estimate the percentual arterial oxygen saturation levels in the capillaries of peripheral vascular beds, known as SpO_2. Thus, pulse oximeters are applied peripherally, for instance, on a fingertip, ear-lope, or forehead (Alian & Shelley, 2022). A healthy person represents an oxygen saturation level of 95% and above (Peterson, 2007). The continuous clinical observation of oxygen saturation levels facilitates prematurely detecting medical conditions such as hypoxemia. Values below healthy levels alert of low oxygen supply to the body’s cells, causing tissue deterioration and life-threatening conditions. Consequently, readings under 70% lead to Values below 70% present low oxygen supply to bodily tissue (Kozier, 2004).

2.2.1 Fundamentals of pulse oximetry

The theoretical background to measuring light absorbance for pulse oximetry is based on the Beer-Lambert law (Wabnitz & Klein, 1999). Simplified, the Beer-Lambert law describes the light attenuation when travelling through a light-absorbing substance. When light enters a medium, a particular portion is transmitted while the other part is absorbed. The theory illustrates that the totality of absorbed or transmitted light equals the incident light. Additionally, it clarifies that the optical path length influences the intensity of light, as it decreases exponentially with the growing distance (Webster, 1997).

To sum up, the Beer-Lambert law describes decreasing light intensity caused by the transmission through a light-absorbing medium as the ratio of emitting and detected light intensity. This ratio exponentially depends on the thickness of the penetrated medium, the concentration, and the extinction coefficient. The extinction coefficient is a measurement of how strongly a medium absorbs light of a specific wavelength (Webster, 1997).

The foundations of pulse oximetry are based on photometric application and the Beer-Lambert law, defining the correlation between a chemical agent's light absorbance behaviour and emitted light. The two core technologies the principle of pulse oximetry derives from are Photoplethysmography (PPG) and Spectrophotometry (Alian & Shelley, 2022). PPG is an optical technology used for describing the change in blood volume (Abay & Kyriacou, 2022). Spectrophotometry measures the intensity of light that transmits a substance. Therefore, light is emitted through a sample, and the amount that passes through is measured (Webster, 1997).

Blood’s oxygen carrier Hb and the pulsatile blood flow are the critical biological factors for pulse oximetry. Pulse oximetry’s principle is based on the light absorbance characteristics of hemoglobin in its oxygenated and deoxygenated state during alternating blood volume. Deoxygenated Hb has a higher absorption affinity in the visible spectrum, specifically close to 660nm. Consequently, oxygenated Hb absorbs more IR light, specified at 940nm, than light from the visible spectrum, specifically red light (Alian & Shelley, 2022). It is evident from previous research and similar studies that these specific wavelengths are commonly used in the manufacturing of pulse oximeters (Alian & Shelley, 2022).

The transmitted light is influenced by blood volume in the blood vessels, which increases during systole and decreases during diastole. When new blood is pumped into the blood vessels during systole, the blood volume rises, increasing light absorption. Consequently, blood volume and light absorption decline to the minimum during diastole, as shown in Figure 2. Hence, two components are considered for the calculation of SpO_2: alternating current (AC) and direct current (DC) (Abay & Kyriacou, 2022).

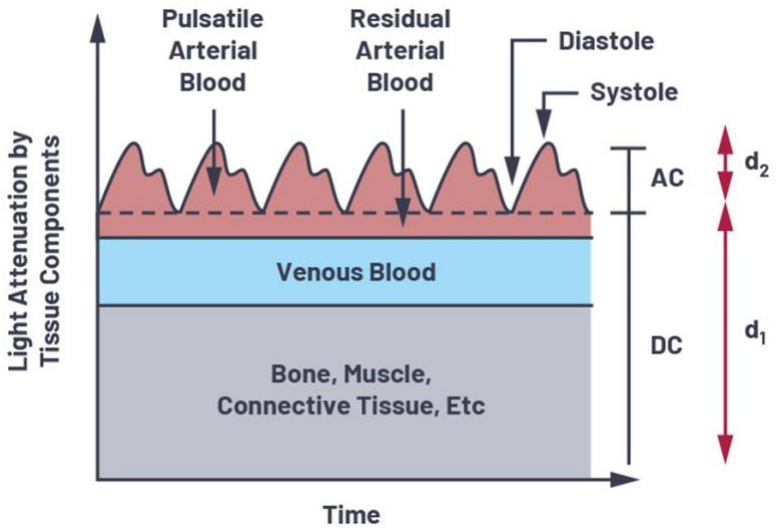

Figure 2: Sectional display of light attenuation through tissue.

Source: (Finnerty, 2022)

DC represents the constant fragment throughout light emission, and AC is the alternating component, illustrating the changing light absorption due to the pulsatile flow (see Fig. 2). In this context, AC is the determination of the SaO_2. Figure 1 furthermore displays that the DC component comprises of the light absorption in the body's integral parts and venous blood. The AC and DC components are obtained for both applied wavelengths, from which a ratio of is calculated (Wabnitz & Klein, 1999). The equation for this calculation is as follows:

$$R = \frac{\frac{ACred}{DCred}}{\frac{ACir}{DCir}}$$

Equation 1: Calculation of the ratio of ratio Source: (Abay & Kyriacou, 2022)

ACred – Alternating current at a wavelength of 660nm

DCred – Direct current at a wavelength of 940nm
ACir – Alternating current at a wavelength of 660nm
DCir – Direct current at a wavelength of 940nm

As mentioned before, the pulsatile flow is a core principle of pulse oximetry, besides the absorption behaviour of hemoglobin. Consequently, a pulse oximeter simultaneously measures the pulse rate.

To sum up, the light absorbance difference of Hb at the specific wavelengths of 660nm and 940nm, is used to determine the peripheral oxygen saturation. It comes together as the ratio of the AC component of each wavelength and the ratio of the DC component of each wavelength. The ratio of ratio will henceforth be referred to as R or simplified, just ratio. Furthermore, a pulse oximeter can detect the pulse by calculating the number of peaks against time.

2.2.2 Technical aspects

Fundamentally a pulse oximeter is comprised of a light source, a detection sensor, signals and algorithms for processing. Conditional to O_2Hb and deoxygenated Hb absorbance behaviour towards red and IR light, a pulse oximeter is constructed of red and IR LEDs. For the detection of the transmitted light, a photodetection sensor is used. A photodetector converts the intensity of light into an electrical current. The transmitted light is captured by a photodetection sensor and digitalised in a microprocessor (Webster, 1997). The technical implementation of a pulse oximeter can be found in detail in chapter three of this thesis.

2.2.3 Calibration methods

The last process of determining a SpO_2 value is dependent on an empirically gained calibration curve. The Beer-Lambert law is not practically achievable due to the influence of light scattering, which is not regarded in the theoretical execution (Wabnitz & Klein, 1999). Hence manufacturers conduct studies on volunteers to relate their manually gained R-values to the equivalent arterial oxygen saturation. Consequently, SpO_2 is a function of R. For the studies, laboratory blood gas analyses are conducted. During the procedures, volunteers are deprived of oxygen while blood is drawn in set time frames to determine oxygen levels in arterial blood

by laboratory methods. Therefore, pulse oximetry is only reliable for SpO_2 values up to 70%. The calibration process results in data specific to the designed pulse oximeter. The data is represented in a calibration curve lodged to the algorithm. The algorithm cross-references every R-value processed with the programmed curve to estimate the SpO_2 output (Wabnitz & Klein, 1999).

2.2.4 Transmissive and reflective model

Commercially available pulse oximeters are commonly built within a finger clip as a transmissive model. However, a second probe type on the market uses the reflective method to determine the SpO_2. The transmissive probe-type works with light sources on one side and a photodetection sensor on the opposite. A reflectance-based probe consists of two LEDs and a photodiode placed on the same side. In the standard transmissive model, light that has not been absorbed by tissue or Hb is detected by the sensor and processed for calculations. The reflectance-based models work by detecting backscattering light and are applied on locations such as the forehead (Webster, 1997).

2.2.5 Accuracy

There are various causes for inducing inaccurate readings of SpO_2. Specific common reasons are revealed in this paragraph.

The accuracy of oxygen saturation readings can be disturbed by multiple internal and external factors, such as ambient light, motion artifact or nail polish (Bowes 3rd, et al., 1989). Internal disruptive factors include physiological conditions of the patient, which could be low perfusion or carbon monoxide inhalation (Peterson, 2007).

Inaccuracy by ambient light is caused due to the sensor's inability to differentiate between light emitted from the LEDs and external light. Due to that, if a pulse oximeter is applied to the surrounding with light of the same wavelengths as the LEDs, ambient light presents to be a noise factor. This can be avoided by covering the device with an opaque material (Peterson, 2007).

Strong movements during testing can cause sensor displacements that lead to another set of inaccurate measurements. Sensor displacement affects the pulse oximeter as the signal is lost and light transmission is disrupted (Wabnitz & Klein, 1999).

Another factor leading to inaccuracy is the dysfunctional hemoglobin derivatives MetHb and COHb. COHb's absorption behaviour is similar to that of O_2Hb. A pulse oximeter cannot distinguish between carbon dioxide and oxygen saturated Hb. If COHb is present in an abnormally high amount, which could lead to carbon monoxide poisoning, a pulse oximeter may present standard readings (Peterson, 2007).

In review, pulse oximetry evaluates the light absorption of hemoglobin when exposed to red and IR light. The ratio to estimate SpO_2 arises by calculating the ratio between constant and alternating components for each applied wavelength. The final computation of the SpO_2 value is dependent on the empirically attained calibration curve, which is used as a reference table to determine SpO_2. The calibration curve interprets as the mathematical relation between R and SpO_2.

2.3 Cephalopod molluscs

This thesis works to develop a medical device for marine animals, such as cephalopod molluscs. Therefore, this section serves as an introduction to the species.

Marine animals of the Antarctic Sea live under extremely low temperatures and thus throughout evolution had to adapt their physiology to this specific habitat. Molluscs are categorized in three classes: cephalopods, snails, and mussels (Jaeckel, 1957). Squid, cuttlefish, and octopus come together as the group of cephalopod molluscs (Mather, et al., 2010).

Unlike vertebrates, many invertebrates' blood transportation is not in a closed circulatory system but in an open system. The circulatory fluid is called hemolymph. There is no distinction in the blood and interstitial fluids (Schaller, et al., 2008). Active invertebrates such as cephalopods blood consist of hemolymphs with leucocytes and the respiratory protein hemocyanin, which is not bound to the blood cells (Jaeckel, 1957).

For the purpose of this thesis, acquiring knowledge about the oxygen-carrier in cephalopod molluscs is of importance. This protein is the hemocyanin and a copper-containing protein found in various cephalopods and other molluscs. Hemocyanin takes on a blue pigment when filled with oxygen. When oxygenated, the hemocyanin takes on a blue colour, while it turns colourless during a reduced or deoxygenated phase (Van Holde, 1995).

From previous research conducted on the Octopus Vulgaris, it is known that the absorbance in oxygenated blood peaks in UV electromagnetic spectrum, specifically at 347nm (Oellermann, et al., 2014). However, further research is needed to attain additional knowledge about hemocyanin's light absorbance behaviour in deoxygenated states.

3. Materials and Method

This chapter of the thesis deals with designing and assembling a prototype oximeter. It gives a detailed explanation of the systematic approach, starting with establishing groundwork, followed by the final assembly.

3.1 Aim and objectives

The aim of this project is to produce a concept for measuring oxygen saturation levels in cephalopods non-invasively. To achieve the target of this project, a proof of concept needs to be established by designing a prototype of a standard pulse oximeter first. The idea is to create the model with elementary electronic components using Arduino, a physical computing program. At last, the developed design concept with Arduino needs to be analysed for feasibility for the initial aim. The overall ambition of this project will be achieved by carrying out the objectives stated below:

- Become acquainted with the Arduino environment.
- Obtain suitable components based on requirements.
- Assemble an operational prototype.
- Customize the calculation for SpO_2.
- Identify measures for system modifications realizable for cephalopods.
- Propose resolution based on theoretical explanations and experimentally acquired knowledge.

3.2 Groundwork

This section comprises a concise introduction to the Arduino environment and descriptions of essential components based on requirements to fulfil the desired performance of pulse oximetry.

3.2.1 Arduino

Arduino is an open-source hardware and software development platform that manufactures boards and small circuits attached with microcontrollers to create interactive projects. Integral parts for creating simple hardware are purchasable in kits, allowing the invention of prototypes for users at different skill levels. The sets include basic electronics, boards, and modules to create easy-to-use hardware (Banzi & Shiloh, 2015). Furthermore, Arduino provides a platform for writing

corresponding software. Programs written with the Arduino Software (IDE), referred to as sketches, can be uploaded to the microcontroller on the board to drive the final hardware. The programming language used is based on C++ (Banzi & Shiloh, 2015). The Arduino language can be categorized into three parts: structure, values, and function. Commands of the category structure are elements of the programming

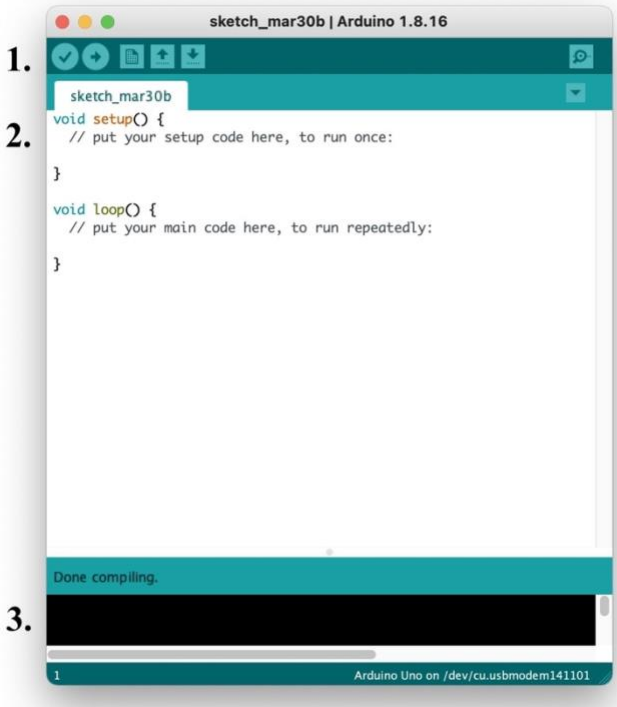

Figure 3: Arduino desktop IDE

language C++, mainly for syntax and operators. Values are commands for defining variables and data types. Commands for controlling the board and executing calculations are assigned to the category function Arduino offers two methods for programming: the online IDE or desktop IDE. Sketches can either be written on a web editor, or the Arduino Software can be downloaded to the terminal. The desktop IDE is a flexible tool that runs on Macintosh OSX, Windows, and Linux (Banzi & Shiloh, 2015).

Figure 3 depicts the desktop IDE structured with a toolbar at the top (1.), a central text editing field (2.), and a commentary section (3.). The first two buttons on the toolbar allow the compilation and uploading of sketches, once initiated, followed by a general sketch verification. Consequently, potential error outputs or other conspicuities are shown in the commentary section. An Arduino sketch is split into two central text bodies: *void setup* and *void loop.* Instructions written within the *setup*

function are executed a single time once the Arduino board is powered. It mainly consists of commands for initializing. The *loop* function is initiated as the setup function is completed and runs the code repeatedly. The instructions written within this function are for the execution of the core tasks of the code. In order to successfully execute the program by enabling the communication between the IDE and the board, the following settings need to be carried out: under the menu option "Tools," the Arduino board used for the project and the port to which the board is connected must be selected. The serial monitor displays the data sent from the board to the computer over a USB connector. It is also essential to choose the baud rate from the drop-down menu on the serial monitor to allow serial communication. The baud rate, conditional to the Arduino board, determines the number of bits of data transmitted per second (Banzi & Shiloh, 2015).

3.2.2 Requirements

Based on the theoretical framework, it is apparent that designated qualifications to create a pulse oximeter must be met. Therefore, the requirements for the electronic components and setting are summarized in this portion:

1. Light source: should be powerful enough to penetrate tissue yet be diminutive to be mounted into casings. The red-light source should have a peak wavelength of 660nm, and the IR light source a peak wavelength of 940nm, as these are the specific wavelengths, where O_2Hb and Hb show absorption.
2. Photodetection sensor: the sensor should be capable of receiving the light of both spectral ranges. Due to the rapid switch between the LEDs during measurements, the sensor should be equipped with a quick response time. Finally, the output signal should be linearly proportional to the intensity of the incident light.
3. Thoughtful alignment of components: for a transmissive-based setup, the red and IR LED should be set on the same side while focusing the part of the LEDs with the most powerful light beam towards the photosensor placed opposite them.
4. System coverage: covering the whole system with means impervious to light.

3.2.3 Components

The Arduino starter pack provides most of the equipment used for this project. Detailed datasheets of the exact content of the kit and individual parts are attached to the appendix (A1). However, other elements compatible with Arduino had to be obtained outside the set to complete the model. The final integral components for the assembling of the prototype are:

Arduino UNO R3

The Arduino UNO R3 board, as illustrated in Figure 4, is the most crucial element for prototyping an object. Besides the mentioned board, Arduino provides users with

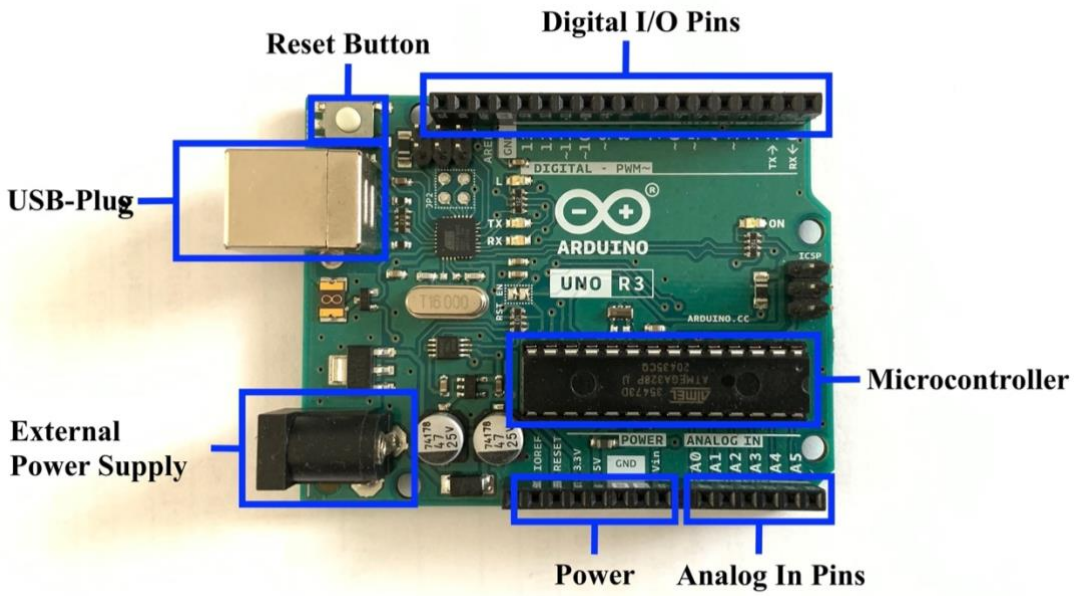

Figure 4: The Arduino UNO R3

numerous other boards. However, these boards will not be described further in this work. Figure 4 furthermore displays the most necessary components of the board. An external power supply can power the board. The USB connection is compulsory for uploading sketches and supplementarily provides the board with power. Besides the powering tools, the UNO R3 provides a reset button, power pins, 14 digital input and output pins, six analog pins, and a microcontroller. The power pins are available as ground, 5V, and 3.3V pins. The digital pins, 0-13, take on a state of only high and low. If the applied voltage exceeds 2,5V, the pin is defined as high. Voltage lesser than that is identified as low. Analog pins, A0-A5, are equipped with an analog-to-digital converter that reads changes in voltage and returns integers between 0 to 1023 proportional to the voltage applied to the analog pins. 0 corresponds to no voltage, while 1023 equals the maximum attainable voltage of 5V. The analog pins'

primary function is to read analog sensors but can likewise be used as digital input and output pins. The supplied current on the pins is set at 40mA.

The microcontroller unit is the focal part of the Arduino boards. Using the IDE, they are programmed to do specific tasks. Its responsibility lies in processing incoming data and facilitating the communication between the Arduino board, hardware components, and serial monitor (Banzi & Shiloh, 2015).

Breadboard

The breadboard is designed with two vertically connected bus strips and two horizontally connected terminal strips, broken in the centre, as Figure 5 illustrates. The bus strips are primarily used for power supply connections and are marked with positive and negative signs. The electoral wiring between all elements is installed using jumper wires.

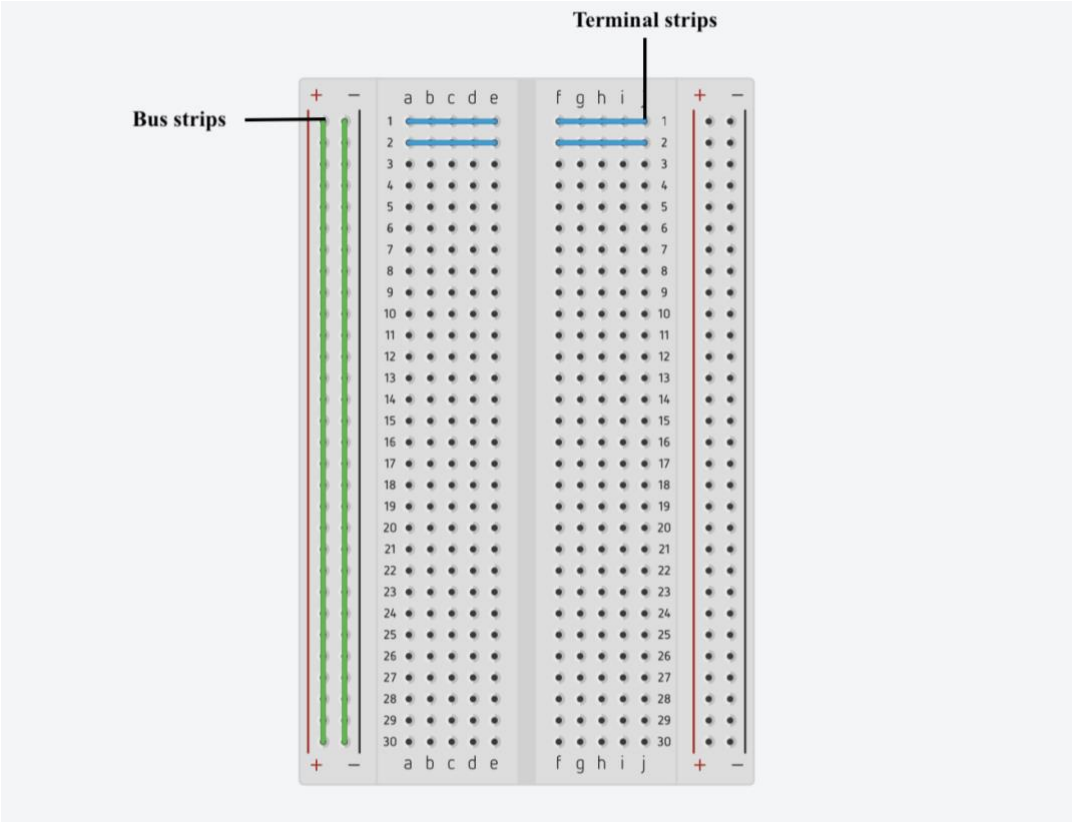

Figure 5: The breadboard

Red LED

The red LED from the Arduino kit has a peak wavelength of 630nm. It should be noted that the red LED comes with a built-in resistor.

Infrared LED (IR333)

An IR LED does not come with the kit and was therefore acquired outside the Arduino kit and has a peak wavelength of 940nm.

Phototransistor (LPT 80A)

The kit does not include a photodetection sensor suitable to the requirements, thus having to be acquired separately. The spectral range sensitivity of the chosen sensor ranges between 450nm and 1100nm, covering both LED wavelength spectra. The response time of the transistor is ten microseconds, guaranteeing a quick reaction to LEDs switching in the millisecond range. The transistor measures the intensity of transmitted light at each wavelength. The value is equivalent to the amount of light the transistor is exposed to.

Resistors

The required resistors for executing the assembly are one 10kΩ resistor, part of the set, and a 330Ω resistor obtained externally.

Miscellaneous

- Jumper wires
- Laptop or computer
- USB cable

Opaque material (e.g., black cloth) or a cardboard box to cover the hardware to protect the system from external interference and other disruptive factors to ensure better performance. Moreover, the coverage should allow enough room for hand movements.

A standard commercially available pulse oximeter for verification during data collection and general reference purposes. For this project, the SPO25 by Sanitas was used. The oximeter of choice was selected free of any specific conditions.

3.3 Assembly

Following the specifications of the formerly introduced components, this subsection describes the composition of the model. The pulse oximeter design of this project is based on the instructions of a prototype oximeter created with the KY-039 heartrate sensor module (Pons, 2020). The initial module is constructed with a photodetection

sensor and an IR LED to measure the heart rate by determining the pulse, precisely as a pulse oximeter detects it. As flexibility in the hardware of this project is indispensable, the prototype will not be created using a pre-manufactured module but rather be built in the same manner with the single components listed above. Nevertheless, the code written for the KY-039 pulse oximeter was adopted for this project.

3.3.1 The Design

The digital plan was developed with Tinkercad, which is a free-of-charge online 3D design platform. The final design of the prototype oximeter is depicted in Figure 6. It serves as a straightforward display of the hardware connections and does not necessarily resemble the actual assembly of the prototype regarding the colours and arrangements of the jumper wires.

Circuit View

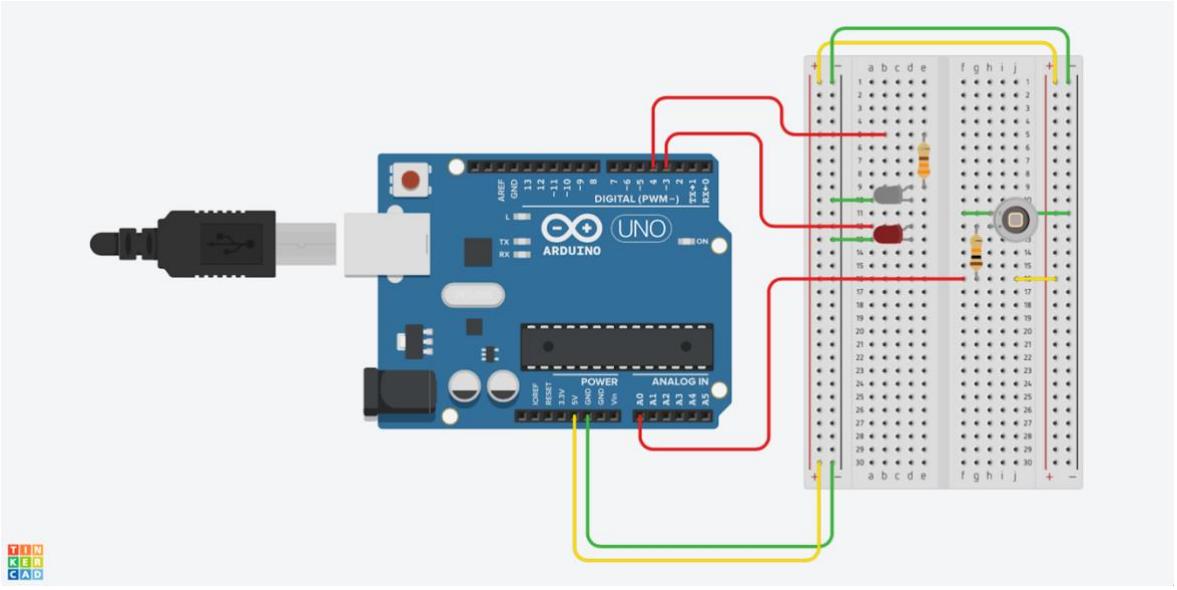

Figure 6: Circuit view of the prototype.

The yellow lines represent the power supply at 5V. The first link is drawn from the board to the first bus strip. Another connection is created between both strips to supply the second bus strip with power. The purpose of this is to provide the components with accessible current on either side to facilitate flexible distributions on the breadboard. The green lines showcase the connection to the GND pin. Both LEDs were positioned on the same side and opposite the LPT 80A phototransistor. The IR LED is connected with the 330Ω resistor and joined to the digital pin D4, and

the red LED is connected to the digital pin D3 (red lines). The software turns the LEDs on and off. Therefore, the light sources do not require a direct power supply. On the right side of the board, the phototransistor is connected over the resistor 10kΩ to the analog pin (A0) to measure the change in voltage during light exposure.

3.3.2 The sketch

The mandatory prerequisite for a pulse oximeter is the software. The software of this prototype is the open-source sketch from the KY-039 oximeter project. Figures 7-9 are chronologically ordered excerpts of the sketch, necessary for understanding how the prototype operates and calculates SpO_2. They will be explained in this section.

```
#define maxperiod_siz 80 // max number of samples in a period
#define measures 10      // number of periods stored
#define samp_siz 4       // number of samples for average
#define rise_threshold 3 // number of rising measures to determine a peak

int T = 20;
int sensorPin = A0;
int REDLed = 3;
int IRLed = 4;
```

Figure 7: Sketch: Declaration of variables

```
void setup() {
  // put your setup code here, to run once:
  Serial.begin(9600);
  Serial.flush();
  pinMode(sensorPin,INPUT_PULLUP);
  pinMode(REDLed,OUTPUT);
  pinMode(IRLed,OUTPUT);

  digitalWrite(REDLed,LOW);
  digitalWrite(IRLed,LOW);

}
```

Figure 8: Sketch: Void setup

The sketch starts with the declaration of essential variables (see Fig. 7) and the initializing of the pins within the void setup function (see Fig. 8). The phototransistor is defined as the sensor pin, while T stands for the period each LED is turned on. Serial.begin() initiates the serial communication, and Serial.flush() clears the serial monitor of previously printed data. With digitalWrite(LOW), both LEDs are turned off at the beginning of the cycle.

Once the setup routine is finished, the core task of the loop function is executed. The LEDs are turned off and on every 20ms in constant change. A photodetector cannot differentiate between red and IR light, wherefore, the LEDs are turned on and off alternately. The phototransistor detects the signals, and the values are saved as integers between 0 and 1023. If all samples of a period, which is limited to 80 samples (see Fig. 7), have been collected, each LED's maximum and minimum values are filtered to calculate the ratio.

```
    R =  ( (REDmax-REDmin) / REDmin) / ( (IRmax-IRmin) / IRmin ) ;
    Serial.println("R= " + String(R));

}
```

Figure 9: Sketch: R calculation

The equation used for calculating the ratio, defined as the variable R in this sketch, is presented in Figure 9. As described in previous chapters, advantageous to the determination of arterial oxygen saturation is the opportunity to measure the pulse simultaneously. In this project's scope, this additional calculation was not excluded; hence the calculation of R is followed by the determination of the pulse, defined as average beats per minute (avBPM).

```
    // SATURTION IS A FUNCTION OF R (calibration)
    // Y = k*x + m
    // k and m are calculated with another oximeter
    int SpO2 = -19 * R + 112;

    if(avBPM > 40 && avBPM <220) Serial.print("avBPM= " + String(avBPM)+" "); else Serial.println("---");

    if(SpO2 > 70 && SpO2 <150) Serial.print("Sp02= " + String(SpO2) + "%"); else Serial.println("---%");

}
```

Figure 10: Sketch: SpO_2 calculation

If at least five reasonable measures are detected, the software is programmed to continue with the SpO_2 calculation (see Fig. 10). This is defined by the variable c. Variable c examines the last ten peaks for values not floating for more than ten percent. If five measures are detected, the calculations are executed. The function that links R with SpO_2 is simplified with: $SpO_2 = K * R + M$. The variables K and M of the equation were calibrated for the KY-039 prototype using a commercially available pulse oximeter. At this point of the project, own data was not available, the SpO2 computation was conducted with the same equation.
Immediately after the calculation is complete, the SpO_2 value and avBPM are printed to the serial monitor by the command Serial.print(). However, the output of the result for SpO_2 is restricted to values above 70% and lesser than 150%.

3.3.3 Data processing

A crucial and final step to finalizing the concept of this prototype was to customize the SpO_2 calculation of the open-source program, as the prototype did not read acceptable values. Consequently, a customised calculation method had to be devised. Conclusively, data had to be collected to execute the closing SpO_2 calculation. The primary condition for this process was working with already completed measurements, as the final estimates had to be done beyond the open-source program.

The first step toward establishing a customised calculation method was calculating the ratio that results in a SpO_2 value of 100%. In the following course of the thesis, the outcome will be referred to as R_{100}.

The next step was to collect data. The optimal approach to gathering statistics was to execute a measurement with the prototype for a certain period while simultaneously conducting a measure with the SPO25.

Figure 11: Measurement method

As depicted in Figure 11, the side-by-side illustration displays the measurement method conducted. The reading with the SPO25 was filmed next to a digital timer, presented on the left half of the image, to associate the values with the output of the serial monitor. For this purpose, the timestamp feature for the serial monitor was activated as it simplified the process of comparing the results of each device. The right half presents results printed to the serial monitor. The output of the serial monitor was later transferred into a text file. Each reading was conducted for three minutes on four test subjects, two female and two male individuals. The ages of the participants vary from 16 to 50 and differ in the thickness of their fingers. At the end of the tests, records of each reading were compiled in an evaluable table (see appendix A4).

The final phase included the manual calculation of the absolute SpO_2 value. Pivotal to the conception of the custom-developed computation were the relatively low R-values printed by the prototype, which obstructed a computation by the initial equation. The customised calculation method for calibration consequently involved the determination of an amplification factor λ, which will be used as the standardized value. This was determined by dividing R_{100} by the lowest R-value of each completed measurement. The data of each reading were split into measuring cycles, each including ten values. The remaining data were not considered during the calculations. From each cycle, the arithmetic average of R rates and SpO_2 values were calculated. Subsequently, the smallest R-value and in connection to this the amplification factor λ were determined. The factor was then each multiplicated by the average R-value of the other measuring cycles, resulting in a new set of R rates. By doing so, the received R-values are multiplicated equally to a higher figure. This calibration process ensures that the prototype's output is aligned to the physical value and the qualitative progression is maintained. At last, the final SpO_2 value can be determined by inserting the newly ascertained ratio into the equation of the sketch. The last step of this procedure was comparing the results to the SPO25 readings. On the base of this, a statement about the functionality and accuracy of the prototype can be made.

Recapitulative, the first four objectives of this project are carried out in the scope of this chapter. The assembly was conducted following the determination of components meeting desired requirements. This is followed by the presentation of the software applied to the prototype. This subchapter is rounded up by exhibiting the measurement and customised calculation methods.

4. Results

This segment focuses on displaying the results from compiling the custom-built hardware and the conducted calculations.

4.1 The prototype pulse oximeter

Figure 12 presents the definite construct of the prototype. Additional illustrations of the hardware are attached to the appendix (A2).

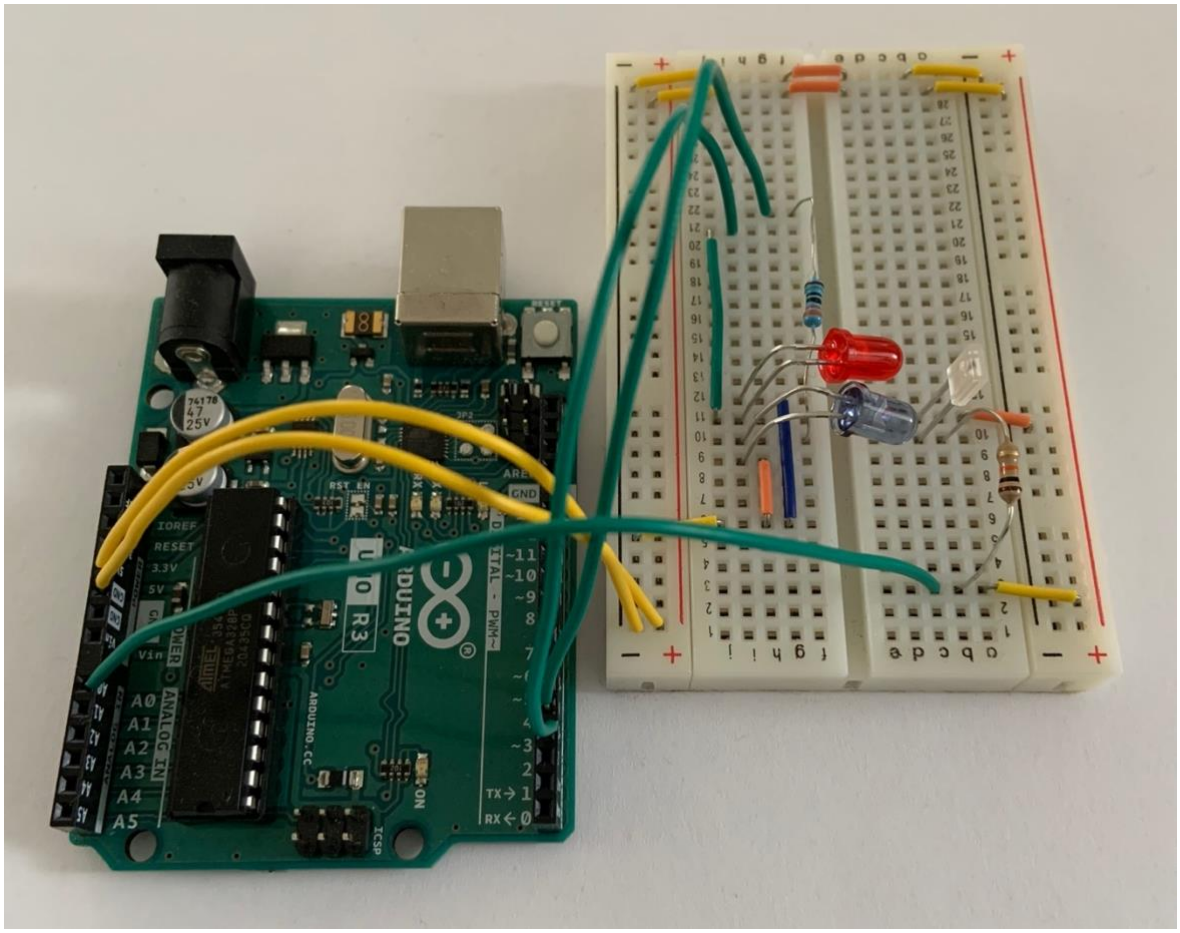

Figure 12: The prototype

4.2 Customised calculations

In pursuance of creating an equation specific and compatible with the developed prototype, analogous changes to the SpO_2 calculation were conducted. Tables 1-3 illustrate the values of the final computations for each reading. R_{100} is a constant value for all measures and was identified as 0,63. As described in the previous chapter, the amplification factor λ was obtained by dividing R_{100} with the lowest R rate of each measure.

Participant one:

The smallest R-value= 0,051

Amplification factor λ= 12

Table 1: Results of participant one.

Measuring cycle	Average R-value	Average SpO_2 value (prototype)	SpO_2 value (SPO25)	New R-value	New SpO_2 value
1.	0,204	108%	98%	2,44	65%
2.	0,288	106%	98%	3,45	46%
3.	0,072	110%	98%	0,86	95%
4.	0,072	110%	98%	0,86	95%
5.	0,051	111%	98%	0,61	100%
6.	0,051	111%	98%	0,61	100%

Participant two:

The smallest R-value = 0,036

Amplification factor λ= 17

Table 2: Results of participant two.

Measuring cycle	Average R-value	Average SpO_2 value (prototype)	SpO_2 value (SPO25)	New R-value	New SpO_2 value
1.	0,044	111%	98%	0,74	97%
2.	0,089	110%	98%	1,51	83%
3.	0,048	111%	98%	0,81	96%
4.	0,081	110%	98%	1,37	85%
5.	0,11	109%	98%	1,87	76%
6. and 7.	0,114	109%	98%	1,93	75%
8.	0,099	110%	98%	1,68	80%
9.	0,069	110%	98%	1,17	89%
10.	0,108	110%	98%	1,83	77%
11.	0,106	110%	98%	1,80	77%
12.	0,113	109%	98%	1,92	75%

13.	0,078	110%	98%	1,32	86%
14.	0,036	111%	98%	0,61	100%
15.	0,044	111%	98%	0,74	97%
16.	0,045	111%	98%	0,76	97%
17.	0,038	111%	98%	0,64	99%
18.	0,049	111%	98%	0,83	96%

Participant three:

The smallest R-value = 0,085

Amplification factor λ= 7

Table 3: Results of participant three.

Measuring cycle	Average R-value	Average SpO_2 value (prototype)	SpO_2 value (SPO25)	New R-value	New SpO_2 value
1.	0,189	108%	-	1,32	86%
2.	0,17	108%	-	1,19	89%
3.	0,138	109%	97%	0,96	93%
4. and 5.	0,119	109%	97%	0,83	96%
6.	0,085	110%	98%	0,59	100%
7.	0,098	110%	98%	0,49	102%
8.	0,149	109%	97%	1,04	92%
9.	0,144	109%	97%	1,00	93%
10.	0,197	108%	97%	1,37	85%
11.	0,194	108%	97%	1,35	86%
12.	0,22	107%	97%	1,54	82%
13.	0,246	107%	97%	1,72	79%
14.	0,241	107%	97%	1,68	80%
15.	0,274	106%	98%	1,91	75%
16.	0,312	106%	98%	2,18	70%

Results of participant four:

There is no recorded data for participant four as the testing was unsuccessful. Despite various attempts to execute accurate readings, the prototype was not capable of receiving utilisable signals. The possible cause for this result will be discussed in the following section.

The variation in measuring cycles for all three participants is caused by temporary pauses during the three-minute readings, as the sensor failed to detect signals. A stabilised measuring was dependent on sensor placement, the overall stability of the system, the participants' steadiness and if contact between sensor and skin or nail was ensured.

Table 4: Pulse rates measured by the prototype and SPO25

Participant 1		Participant 2		Participant 3	
BPM Prototype	BPM Sanitas	BPM Prototype	BPM Sanitas	BPM Prototype	BPM Sanitas
73	75	66	67	92	85
74	75	69	67	82	84
75	75	69	67	82	84
75	75	67	67	82	84
75	74	66	67	81	82
74	73	62	66	81	82
75	73	61	67	82	82
76	73	61	67	83	82
86	73	61	67	83	82
86	73	63	67	82	82

Table 4 illustrates the pulse rate measured by the prototype and Sanitas SPO25 in direct comparison. In contrast to the SpO2 values, the pulse rate measured by the prototype does not deviate from the reading with the SPO25.

A comprehensive discussion follows this chapter, thematically broaching this thesis's systematic approach and outcomes and the final two objectives of realizing a concept for cephalopods and proposing possible resolutions.

5. Discussion

This chapter deals with the analysis of the execution of the thesis and the presented results. Additionally, the last two objectives to achieve the aim of this thesis are discussed.

5.1 Execution of the project

Within this subchapter, the acquired results are analysed in relation to the systematic approach of this thesis.

Based on the output of the low R-values during measurements, it quickly became apparent that the initial SpO_2 equation needed to be changed. There are two significant possible sources of errors instigating the undesirable R rates, the focal component for computing a SpO_2 value. The first cause is immense light scattering because the light of the LEDs passes the phototransistor on the side. The other source is the phototransistor's sensitivity toward the red LED. Even though the sensor covers the spectral range of red light, its sensitivity is almost 50% less than the IR light, which is illustrated on the phototransistor datasheet (see appendix A1). Consequently, the light from the red LED is not perceived fully due to the scattering and the lower absorption from the sensor.

A calculation process was developed to manage the output of SpO_2 values. This required an adjustment to the software equation. The equation from the open-source sketch was manually calibrated with R values specific to the KY-039 oximeter.
The KY-039 prototype and the prototype of the thesis differ in their construct and components. The KY-039, a module aimed to measure the heartrate, was converted into a pulse oximeter prototype. The module comes with a photodetection sensor and an IR LED. For the modification, a red LED was added to the circuit with a corresponding resistor. Finally, the complete system was added into a self-made casing. In comparison, the prototype of this thesis was built freely on a breadboard with separately purchased components, different to the KY-039 prototype.

However, the output of R values of the prototype of this project disclosed that either the R rates or the SpO_2 values had to be corrected. However, the initial step was to confirm the circuit of the prototype to exclude errors produced by the prototype. The

construct of the hardware was checked repeatedly and approved by an electrical engineering professor at the university in Bremerhaven. As a result, a solution approach was developed to increase the R-values for the accurate SpO_2 reading.

The solution approach to determine the final SpO_2 values were rather unconventional, as the prototype brought restrictions due to which a complete computation by the software was not executable. The sensitivity of the construct caused meagre R rates. The equation used in the software was determined experimentally to its corresponding KY-039 hardware. Hence, the R-values of the thesis prototype and the equation do not work together. Therefore, the idea was to create a customised calibration, which included the manual calculation of the SpO_2 value. The personalized calibration method aimed to obtain reasonable SpO_2 values without additional discrepancies due to the hardware's instability. Other than that, the objective was to show the system's adaptability to accomplish the initial aim of the thesis despite the unequal SpO_2 readings. The process is based on calibrating the system by standardization, a method often used in electrical engineering. The process helps tailor the existing figure to its physical value. For standardization, the required value is aligned to the maximum value, and every subsequent output is proportionally lower than the maximum value. This process was completed to ensure the qualitative progression of the results. The maximum value is the output that gives a SpO_2 value of 100%. From the theory of pulse oximetry, it is known that, as the ratio rises, the SpO_2 value decreases. As a result, the maximum SpO_2 value corresponds to the lowest R-value. The reason for doing the calculation in measuring cycles, with ten values each, was to overcome strongly fluctuating figures. This was achieved by calculating the arithmetic mean for every cycle.

When looking at the results, it is of importance that the final SpO_2 value is based on secondary calibration. The equation itself was determined through calibration, which was used to calculate calibrated values. Consequently, it is evident that the results will most likely differ from the reference SpO_2 value. However, the new R-values of all measurements present to be reasonable and are expected rates for a pulse oximeter. The different R-values of each measurement imply that the prototype is functional, as the sensor is reactive to the variation of incoming signals.

Nevertheless, there are more interferences than outputs of accurate R-values caused by the previously stated reasons. Missing results for the last participant can be caused by the test subjects' tremor. Due to that, the system could most likely not find enough suitable measures to calculate SpO_2 values. Comparing the results of SpO2 values in Tables 1-3, it Is evident that the newly calculated fluctuate immensely and differ from the steady readings of the SPO25. Whereas the initial SpO_2 values by the prototype are comparatively steady. Additionally, they only differ from the SPO25 readings in a smaller range. Based on this, the standardization method by customized calibration seems ineffective and does not better the final SpO_2 values.

The limitation of movement affected the possibilities of data collection and the results. Performing different testing scenarios were not achievable, as both devices would need to be exposed to the same testing conditions. However, due to the already low R-values and every now and then fluctuating rates, the interpretation of the output would have been challenging. The changes in the output would not have been apparent. Furthermore, the prototype needed support several times due to the instability and adjusting the LEDs to the participant's varying finger sizes. Thus, both devices had to be kept in a resting position, resulting in a continuously constant value from the SPO25.

Implementing the hardware into a finger clip appears to be a good way of enhancing the R-values. It creates stability, and the light of LEDs can be concentrated directly on the sensor. The current installation only allows the sensor to detect half of the light range, as the light can escape into the surrounding air space. This adjustment would enable intensive testing, by which a specified calibration equation can be established for this prototype. Conducting stabilised measurements will also allow assessing the accuracy of the prototype.
Additionally, finding a transistor proportional to the size of the LEDs could likewise improve the final outputs, as the detection field is consequently more significant. The phototransistor was chosen based on the main requirement of covering the spectral range needed, wherefore, the size of the component was not regarded.

Despite the described difficulties, there is one aspect proving the system's functionality. That is the pulse rate, which was simultaneously measured by the system. The pulse rate calculation depends on the number of beats during the pulsatile blood flow in the artery for a given period. It is independent of the calculation of R as no ratio must be calculated. At last, the pulse rate is printed as an average of five decent measures. When comparing the values of the prototype to the output of the SPO25, the results are alike, as illustrated in Table 4. The values occasionally deviate but generally produce the same results.

To sum up, the selected components and the customised processing allowed the development of functional hardware. Nevertheless, the results are poor and require improvement by enhancing the prototype structure to reduce noise. Hardware implemented into a strong casing provides stability and flexibility, which could improve testing techniques, resulting in versatile and reasonable, reproducible data.

5.2 Methodical approach for system modification

This segment points out the prerequisites for creating a model appliable on cephalopods based on the custom-built prototype and discusses a possible execution approach.

Considering the physiology of cephalopods, the construct of a standard transmissive-based pulse oximeter is not ideal as a model for cephalopod molluscs. A transmissive model is most effective when applied to tissues of small thickness that are simpler to grip by a probe. Based on the point presented, it can be said that a reflectance-based concept is beneficial when creating a model for cephalopods, especially when considering the uncomplicated application on cephalopods' bodies. For a reflectance setup, applying multiple photodiodes could be advantageous because a higher quantity of backscattering light can be detected when placed with respect to each other. The more backscattered light is seen, the larger the plethysmograph can be. In addition, the utilisation of multiple sensors, each covering specific wavelengths, effectively pre-empts the problem of applying one sensor, with a broad-spectrum range, with less sensitivity toward one wavelength.

Research conducted in the scope of this thesis indicates that the market for electronic components for the UV-VIS range is not broadly based. Electronics that

can be attained are not similar to the components used for the prototype. However, sensors and possible LEDs available are flat models, which supports the idea of creating a reflectance-based model.

Since the customised calculations displayed adaptability in the pulse oximeter concept, this model can achieve the same. However, this needs extensive testing, which will prove to be difficult as testing during development cannot be performed on cephalopods themselves. Although testing on their blood will give relative oxygen concentration value, it is required to assess the additional constant value absorbed due to bodily tissues to determine absolute blood oxygen saturation level.

6. Conclusion

This chapter will conclude the thesis by reviewing the key findings in relation to the research goals. Moreover, it will outline their value and contributions and present opportunities for future research purposes.

In review, the thesis on hand aimed to investigate a concept to measure blood oxygen levels in cephalopods. For this purpose, a standard pulse oximeter was replicated with the Arduino development environment. The main objective of this process was to develop a proof of concept by building the oximeter with common electronic components. Based on this, the objective was to identify and propose measures for reasonable modifications to enable pulse oximetry on cephalopod molluscs.

The results of the transmissive-based concept clearly illustrate the system's functionality but simultaneously raise the question of accuracy. Due to sources of errors, the final output of the SpO_2 was not reliable. A customised calibration method was developed to gain reliable predictions on the custom-built prototype and demonstrate adaptability.

The outcome presented reasonable R-values with corresponding SpO_2 outputs, however with larger deviations, making the calculations ineffective. As a result, it can be concluded that henceforth, the focus should be put on increasing the R-values by optimising the prototype. Through the discovery of sources of error provided by the prototype, new insights regarding the adaptation for cephalopods were gained. The most significant finding implies that in order to actualise a practical pulse oximeter for cephalopods, researchers need to create a reflectance-based model with multiple photodetection sensors and consequently avoid the limiting factor of using a single sensor to cover a broad-spectrum range.

Finally, the evaluation of the results implies that a proof of concept for the custom-built prototype is achieved and a possibility of practical implementation on cephalopods is achievable by developing a reflectance-based model.

Future researchers should consider building a firm casing for the developed prototype to establish a SpO_2 equation specific to it, bypassing the manual calculation. Further research is needed to determine absorption behaviour in cephalopod tissue and the oxygen-carrier hemocyanin to finalise suitable components. Subsequently, the concept developed in this thesis can be applied to constructing a prototype concept suitable for cephalopods.

Bibliography

Abay, T. Y. & Kyriacou, P. A., 2022. Photoplethysmography. In: P. Kyriacou & J. Allen, Hrsg. *5 - Photoplethysmography in oxygenation and blood volume measurments.* s.l.:Academic Press, pp. 147-188.

Alian, A. A. & Shelley, K. H., 2022. Photoplethysmography. In: *10 - PPG in clinical monitoring.* s.l.:Academic Press, pp. 341-359.

Alfred-Wegener-Institut, 2021. *awi.* [Online]
Available at: https://www.awi.de/ueber-uns/organisation/profil.html [Accessed 15 02 2022]

Association, H. S., 2022. *hsa.org.* [Online]
Available at: https://www.hsa.org.uk/about/about [Accessed 15 02 2022].

Banzi, M. & Shiloh, M., 2015. *Make: Getting Started with Arduino.* 3. ed. s.l.:Maker Media, Inc.

Brandes, R., Lang, F. & Schmidt, R. F., 2019. *Physiologie des Menschen.* s.l.:Springer.

Bright, H. K., 2018. *OU Human Physiology Textbook.* s.l.:ObenStax CNX.

Bowes 3rd, W., Corke, B. A. & Hulka, J., 1989. Pulse oximetry: a review of the theory, accuracy and clinical applications.. *Obstetrics and Gynecology,* 74(3), pp. 541-546.

CephRes, 2022. *cephalopodresearch.* [Online]
Available at: https://www.cephalopodresearch.org/cephres-factsheet/ [Accessed 15 02 2022].

Finnerty, R. Light, (2022). Sectional display of light attenuation through tissue. [Drawing] https://www.analog.com/en/technical-articles/how-to-design-a-better-pulse-oximeter.html

Heather KetchumEric Bright, OU Human Physiology Textbook. OpenStax CNX. 6 Jul 2017 http://cnx.org/contents/48d9cf34-dcfd-4dd3-a196-eec3eea6f408@1.9.

Jaeckel, S. H., 1957. *Kopffüsser (Tintenfische).* s.l.:Ziemsen.

Mather, J. A., Anderson, R. C. & Wood, J. B., 2010. *Octopus.* s.l.:Timber Press.

Oellermann, M., Pörtner, H.-O. & Mark, F. C., 2014. Simultaneous high-resolution pH and spectrophotometric recordings of oxygen binding in blood microvolumes. *The Journals of Experimental Biology,* Issue 217, pp. 1430-1436.

OpenStax, 2013. *openstax.* [Online]
Available at: https://openstax.org/books/anatomy-and-physiology/pages/18-3-erythrocytes#fig-ch19_03_03 [Accessed 03 03 2022].

Perutz, M. F., 1978. Hemoglobin Structure and Respiratory Transport. *Scientific American,* 239(6), pp. 92-125.

Peterson, B. K., 2007. Chapter 22 - Vital Signs. In: M. H. Cameron & L. G. Monroe, eds. *Physical Rehabilittion.* s.l.:W. B. Saunders, pp. 598-624.

Pons, G., 2020. *arduino.* [Online]
Available at: https://create.arduino.cc/projecthub/giulio-pons/really-homemade-oximeter-sensor-7cf6a1?ref=similar&ref_id=407490&offset=4 [Accessed 01 12 2021].

Salewski, C., 2022. *awi.* [Online]
Available at: https://www.awi.de/ueber-uns/organisation/alfred-wegener.html [Accessed 15 02 2022].

Schaller, J. et al., 2008. *Human Blood Plasma Proteins: Structure and Function.* s.l.:John Wiley & Sons, Ltd.

Schneider, M. & Rein, H., 1971. *Einführung in die Physiologie des Menschen.* s.l.:Springer.

Koecke, H. U., 1975. *Allgemeine Biologie für Mediziner & Biologen.* s.l.:F. K. Schattauer Verlag.

Kozier, B., Berman, A., Erb, G. L., & Snyder, S. (2004). *Kozier & Erb's techniques in clinical nursing: Basic to intermediate skills*. Prentice Hall.

Van Holde, K. M. K. I., 1995. Advances in Protein Chemistry. In: *Hemocyanin.* s.l.:Academic Press, pp. 1-81.

Wabnitz, H. & Klein, K.-D., 1999. *Pulsoximeter - Messtechnische Prüfung von Medizinprodukten mit Messfunktion (4).* s.l.:Wirtschaftsverlag NW.

Webster, J. G., 1997. *Design of Pulse Oximeters.* s.l.:Institute of Physics Publishing Ltd.

Appendix

A.1 Datasheets

ARDUINO

THE ARDUINO STARTER KIT

Everything you need for your firs Arduino projects

The kit includes:

1	Arduino Projects Book (170 pages)
1	Arduino UNO board rev.3
1	USB cable 1 Breadboard
1	Easy-to-assemble wooden base
1	9v battery snap
70	Solid core jumper wires
2	Stranded jumper wires
6	Photoresistor [VT90N2 LDR]
3	Potentiometer 10kilohm
10	Pushbuttons
1	Temperature sensor [TMP36]
1	Tilt sensor
1	LCD alphanumeric (16x2 characters)
1	LED (bright white)
1	LED (RGB – common cathode)
8	LEDs (red)
8	LEDs (green)
8	LEDs (yellow)
3	LEDs (blue)
1	Small DC motor 6/9V
1	Small servo motor
1	Piezo capsule [PKM17EPP-4001-B0]
1	H-bridge motor driver [L293D]
2	Optocouplers [4N35]
5	Transistor [BC547]
2	Mosfet transistors [IRF520]
5	Capacitors 100nF
3	Capacitors 100uF
5	Capacitor 100pF
5	Diodes [1N4007]
3	Transparent gels (red, green, blue)
1	Male pins strip (40x1)
20	Resistors 220 ohm
5	Resistors 560 ohm
5	Resistors 1 kilohm
5	Resistors 4.7 kilohm
10	Resistors 10 kilohm
5	Resistors 1 megohm
5	Resistors 10 megohm

For more information **arduino.cc/starterkit**

WARNING: CHOKING HAZARD This products contains small parts and should be kept out of the reach of children under the age of 3, because the parts or their pieces may presents a chocking hazard to small children.

CAUTION This is an educational product, not a toy. It's not intended for children under 8 years old.

Product Reference Manual
SKU: A000066

Description

The Arduino UNO R3 is the perfect board to get familiar with electronics and coding. This versatile microcontroller is equipped with the well-known ATmega328P and the ATMega 16U2 Processor.
This board will give you a great first experience within the world of Arduino.

Target areas:

Maker, introduction, industries

X

Features

- **ATMega328P** Processor
  - **Memory**
    - AVR CPU at up to 16 MHz
    - 32KB Flash
    - 2KB SRAM
    - 1KB EEPROM
  - **Security**
    - Power On Reset (POR)
    - Brown Out Detection (BOD)
  - **Peripherals**
    - 2x 8-bit Timer/Counter with a dedicated period register and compare channels
    - 1x 16-bit Timer/Counter with a dedicated period register, input capture and compare channels
    - 1x USART with fractional baud rate generator and start-of-frame detection
    - 1x controller/peripheral Serial Peripheral Interface (SPI)
    - 1x Dual mode controller/peripheral I2C
    - 1x Analog Comparator (AC) with a scalable reference input
    - Watchdog Timer with separate on-chip oscillator
    - Six PWM channels
    - Interrupt and wake-up on pin change
  - **ATMega16U2 Processor**
    - 8-bit AVR® RISC-based microcontroller
  - **Memory**
    - 16 KB ISP Flash
    - 512B EEPROM
    - 512B SRAM
    - debugWIRE interface for on-chip debugging and programming
  - **Power**
    - 2.7-5.5 volts

1 The Board

1.1 Application Examples

The UNO board is the flagship product of Arduino. Regardless if you are new to the world of electronics or will use the UNO as a tool for education purposes or industry-related tasks.

First entry to electronics: If this is your first project within coding and electronics, get started with our most used and documented board; Arduino UNO. It is equipped with the well-known ATmega328P processor, 14 digital input/output pins, 6 analog inputs, USB connections, ICSP header and reset button. This board includes everything you will need for a great first experience with Arduino.

Industry-standard development board: Using the Arduino UNO board in industries, there are a range of companies using the UNO board as the brain for their PLC's.

Education purposes: Although the UNO board has been with us for about ten years, it is still widely used for various education purposes and scientific projects. The board's high standard and top quality performance makes it a great resource to capture real time from sensors and to trigger complex laboratory equipment to mention a few examples.

1.2 Related Products

- Starter Kit
- Tinkerkit Braccio Robot
- Example

2 Ratings

2.1 Recommended Operating Conditions

Symbol	Description	Min	Max
	Conservative thermal limits for the whole board:	-40 °C (-40°F)	85 °C (185°F)

NOTE: In extreme temperatures, EEPROM, voltage regulator, and the crystal oscillator, might not work as expected due to the extreme temperature conditions

2.2 Power Consumption

Symbol	Description	Min	Typ	Max	Unit
VINMax	Maximum input voltage from VIN pad	6	-	20	V
VUSBMax	Maximum input voltage from USB connector		-	5.5	V
PMax	Maximum Power Consumption	-	-	xx	mA

3 Functional Overview

3.1 Board Topology

Top view

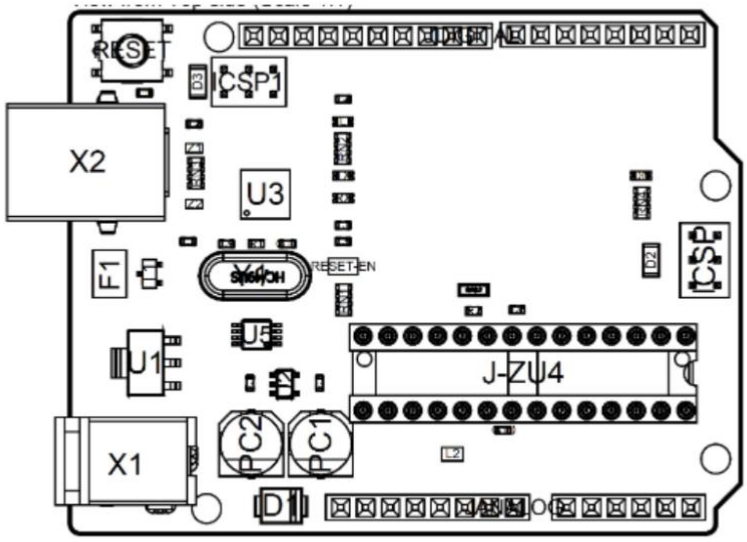

Board topology

Ref.	Description	Ref.	Description
X1	Power jack 2.1x5.5mm	U1	SPX1117M3-L-5 Regulator
X2	USB B Connector	U3	ATMEGA16U2 Module
PC1	EEE-1EA470WP 25V SMD Capacitor	U5	LMV358LIST-A.9 IC
PC2	EEE-1EA470WP 25V SMD Capacitor	F1	Chip Capacitor, High Density
D1	CGRA4007-G Rectifier	ICSP	Pin header connector (through hole 6)
J-ZU4	ATMEGA328P Module	ICSP1	Pin header connector (through hole 6)
Y1	ECS-160-20-4X-DU Oscillator		

3.2 Processor

The Main Processor is a ATmega328P running at up tp 20 MHz. Most of its pins are connected to the external headers, however some are reserved for internal communication with the USB Bridge coprocessor.

3.3 Power Tree

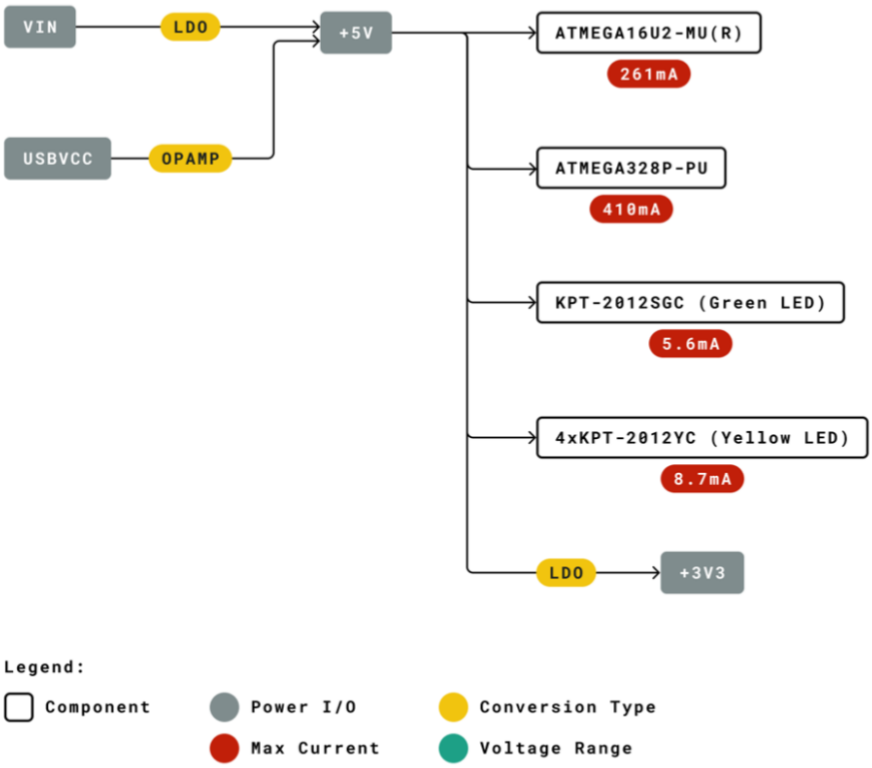

Power tree

4 Board Operation

4.1 Getting Started - IDE

If you want to program your Arduino UNO while offline you need to install the Arduino Desktop IDE [1] To connect the Arduino UNO to your computer, you'll need a Micro-B USB cable. This also provides power to the board, as indicated by the LED.

4.2 Getting Started - Arduino Web Editor

All Arduino boards, including this one, work out-of-the-box on the Arduino Web Editor [2], by just installing a simple plugin.

The Arduino Web Editor is hosted online, therefore it will always be up-to-date with the latest features and support for all boards. Follow **[3]** to start coding on the browser and upload your sketches onto your board.

4.3 Getting Started - Arduino IoT Cloud

All Arduino IoT enabled products are supported on Arduino IoT Cloud which allows you to Log, graph and analyze sensor data, trigger events, and automate your home or business.

4.4 Sample Sketches

Sample sketches for the Arduino XXX can be found either in the "Examples" menu in the Arduino IDE or in the "Documentation" section of the Arduino Pro website [4]

4.5 Online Resources

Now that you have gone through the basics of what you can do with the board you can explore the endless possibilities it provides by checking exciting projects on ProjectHub **[5]**, the Arduino Library Reference **[6]** and the online store **[7]** where you will be able to complement your board with sensors, actuators and more

4.6 Board Recovery

All Arduino boards have a built-in bootloader which allows flashing the board via USB. In case a sketch locks up the processor and the board is not reachable anymore via USB it is possible to enter bootloader mode by double-tapping the reset button right after power up.

5 Connector Pinouts

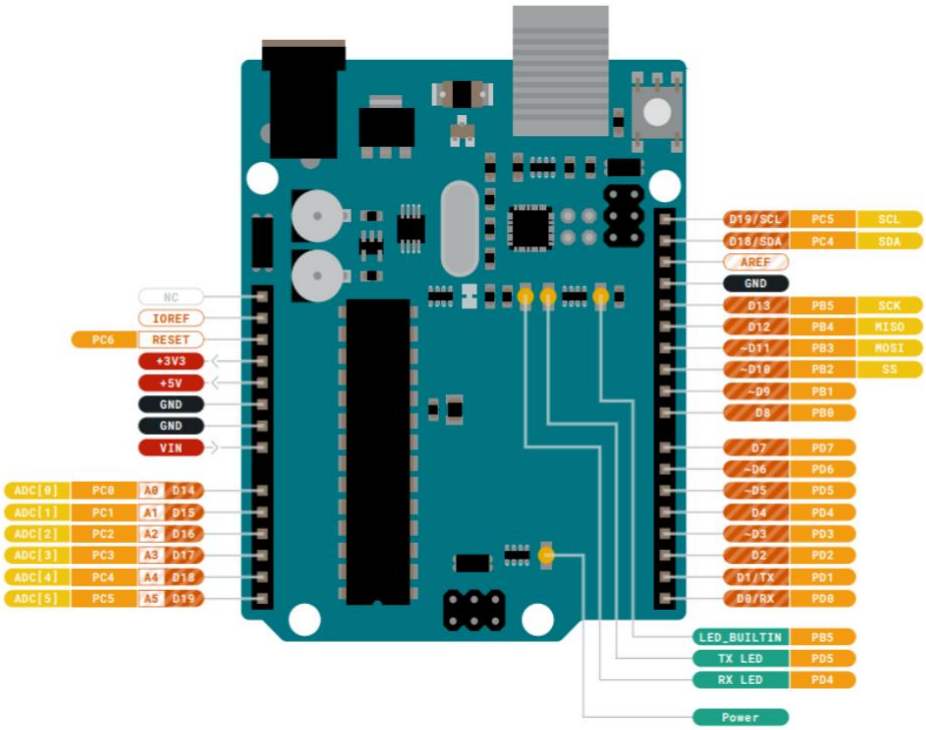

Pinout

5.1 JANALOG

Pin	Function	Type	Description
1	NC	NC	Not connected
2	IOREF	IOREF	Reference for digital logic V - connected to 5V
3	Reset	Reset	Reset
4	+3V3	Power	+3V3 Power Rail
5	+5V	Power	+5V Power Rail
6	GND	Power	Ground
7	GND	Power	Ground
8	VIN	Power	Voltage Input
9	A0	Analog/GPIO	Analog input 0 /GPIO
10	A1	Analog/GPIO	Analog input 1 /GPIO
11	A2	Analog/GPIO	Analog input 2 /GPIO
12	A3	Analog/GPIO	Analog input 3 /GPIO
13	A4/SDA	Analog input/I2C	Analog input 4/I2C Data line
14	A5/SCL	Analog input/I2C	Analog input 5/I2C Clock line

5.2 JDIGITAL

Pin	Function	Type	Description
1	D0	Digital/GPIO	Digital pin 0/GPIO
2	D1	Digital/GPIO	Digital pin 1/GPIO
3	D2	Digital/GPIO	Digital pin 2/GPIO
4	D3	Digital/GPIO	Digital pin 3/GPIO
5	D4	Digital/GPIO	Digital pin 4/GPIO
6	D5	Digital/GPIO	Digital pin 5/GPIO
7	D6	Digital/GPIO	Digital pin 6/GPIO
8	D7	Digital/GPIO	Digital pin 7/GPIO
9	D8	Digital/GPIO	Digital pin 8/GPIO
10	D9	Digital/GPIO	Digital pin 9/GPIO
11	SS	Digital	SPI Chip Select
12	MOSI	Digital	SPI1 Main Out Secondary In
13	MISO	Digital	SPI Main In Secondary Out
14	SCK	Digital	SPI serial clock output
15	GND	Power	Ground
16	AREF	Digital	Analog reference voltage
17	A4/SD4	Digital	Analog input 4/I2C Data line (duplicated)
18	A5/SD5	Digital	Analog input 5/I2C Clock line (duplicated)

5.3 Mechanical Information

5.4 Board Outline & Mounting Holes

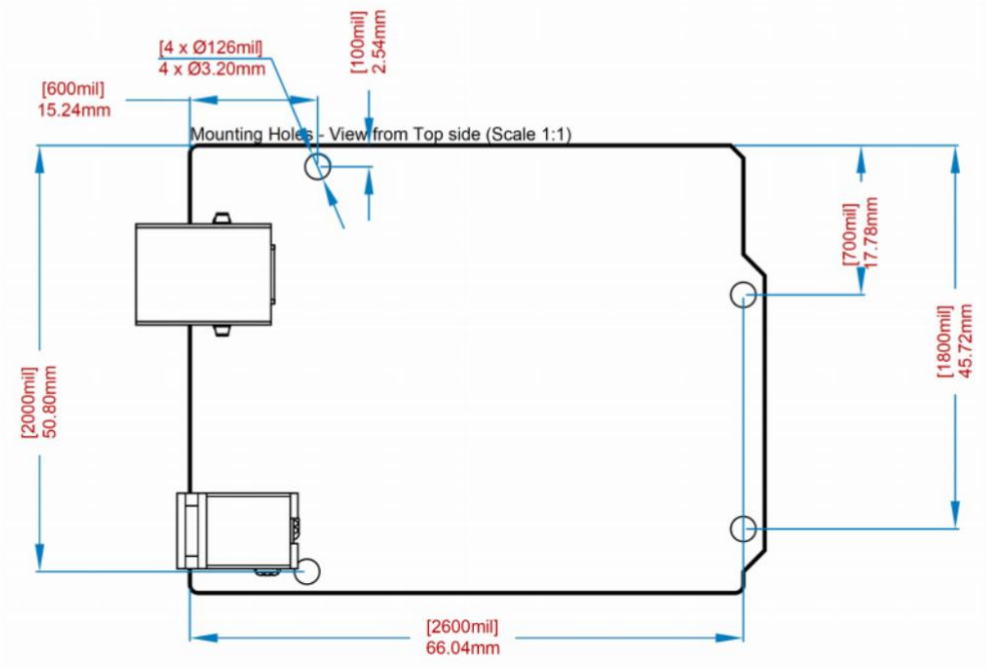

Board outline

6 Certifications

6.1 Declaration of Conformity CE DoC (EU)

We declare under our sole responsibility that the products above are in conformity with the essential requirements of the following EU Directives and therefore qualify for free movement within markets comprising the European Union (EU) and European Economic Area (EEA).

ROHS 2 Directive 2011/65/EU	
Conforms to:	EN50581:2012
Directive 2014/35/EU. (LVD)	
Conforms to:	EN 60950-1:2006/A11:2009/A1:2010/A12:2011/AC:2011
Directive 2004/40/EC & 2008/46/EC & 2013/35/EU, EMF	
Conforms to:	EN 62311:2008

6.2 Declaration of Conformity to EU RoHS & REACH 211 01/19/2021

Arduino boards are in compliance with RoHS 2 Directive 2011/65/EU of the European Parliament and RoHS 3 Directive 2015/863/EU of the Council of 4 June 2015 on the restriction of the use of certain hazardous substances in electrical and electronic equipment.

Substance	Maximum limit (ppm)
Lead (Pb)	1000
Cadmium (Cd)	100
Mercury (Hg)	1000
Hexavalent Chromium (Cr6+)	1000
Poly Brominated Biphenyls (PBB)	1000
Poly Brominated Diphenyl ethers (PBDE)	1000
Bis(2-Ethylhexyl} phthalate (DEHP)	1000
Benzyl butyl phthalate (BBP)	1000
Dibutyl phthalate (DBP)	1000
Diisobutyl phthalate (DIBP)	1000

Exemptions: No exemptions are claimed.

Arduino Boards are fully compliant with the related requirements of European Union Regulation (EC) 1907 /2006 concerning the Registration, Evaluation, Authorization and Restriction of Chemicals (REACH). We declare none of the SVHCs (https://echa.europa.eu/web/guest/candidate-list-table), the Candidate List of Substances of Very High Concern for authorization currently released by ECHA, is present in all products (and also package) in quantities totaling in a concentration equal or above 0.1%. To the best of our knowledge, we also declare that our products do not contain any of the substances listed on the "Authorization List" (Annex XIV of the REACH regulations) and Substances of Very High Concern (SVHC) in any significant amounts as specified by the Annex XVII of Candidate list published by ECHA (European Chemical Agency) 1907 /2006/EC.

6.3 Conflict Minerals Declaration

As a global supplier of electronic and electrical components, Arduino is aware of our obligations with regards to laws and regulations regarding Conflict Minerals, specifically the Dodd-Frank Wall Street Reform and Consumer Protection Act, Section 1502. Arduino does not directly source or process conflict minerals such as Tin, Tantalum, Tungsten, or Gold. Conflict minerals are contained in our products in the form of solder, or as a component in metal alloys. As part of our reasonable due diligence Arduino has contacted component suppliers within our supply chain to verify their continued compliance with the regulations. Based on the information received thus far we declare that our products contain Conflict Minerals sourced from conflict-free areas.

7 FCC Caution

Any Changes or modifications not expressly approved by the party responsible for compliance could void the user's authority to operate the equipment.

This device complies with part 15 of the FCC Rules. Operation is subject to the following two conditions:

(1) This device may not cause harmful interference

(2) this device must accept any interference received, including interference that may cause undesired operation.

FCC RF Radiation Exposure Statement:

1. This Transmitter must not be co-located or operating in conjunction with any other antenna or transmitter.
2. This equipment complies with RF radiation exposure limits set forth for an uncontrolled environment.
3. This equipment should be installed and operated with minimum distance 20cm between the radiator & your body.

English: User manuals for license-exempt radio apparatus shall contain the following or equivalent notice in a conspicuous location in the user manual or alternatively on the device or both. This device complies with Industry Canada license-exempt RSS standard(s). Operation is subject to the following two conditions:

(1) this device may not cause interference

(2) this device must accept any interference, including interference that may cause undesired operation of the device.

French: Le présent appareil est conforme aux CNR d'Industrie Canada applicables aux appareils radio exempts de licence. L'exploitation est autorisée aux deux conditions suivantes :

(1) l' appareil nedoit pas produire de brouillage

(2) l'utilisateur de l'appareil doit accepter tout brouillage radioélectrique subi, même si le brouillage est susceptible d'en compromettre le fonctionnement.

IC SAR Warning:

English This equipment should be installed and operated with minimum distance 20 cm between the radiator and your body.

French: Lors de l' installation et de l' exploitation de ce dispositif, la distance entre le radiateur et le corps est d 'au moins 20 cm.

Important: The operating temperature of the EUT can't exceed 85°C and shouldn't be lower than -40°C.

Hereby, Arduino S.r.l. declares that this product is in compliance with essential requirements and other relevant provisions of Directive 2014/53/EU. This product is allowed to be used in all EU member states.

8 Company Information

Company name	Arduino S.r.l
Company Address	Via Andrea Appiani 25 20900 MONZA Italy

9 Reference Documentation

Reference	Link
Arduino IDE (Desktop)	https://www.arduino.cc/en/Main/Software
Arduino IDE (Cloud)	https://create.arduino.cc/editor
Cloud IDE Getting Started	https://create.arduino.cc/projecthub/Arduino_Genuino/getting-started-with-arduino-web-editor-4b3e4a
Arduino Pro Website	https://www.arduino.cc/pro
Project Hub	https://create.arduino.cc/projecthub?by=part&part_id=11332&sort=trending
Library Reference	https://www.arduino.cc/reference/en/
Online Store	https://store.arduino.cc/

10 Revision History

Date	Revision	Changes
xx/06/2021	1	Datasheet release

EVERLIGHT

Technical Data Sheet

5mm Infrared LED , T-1 3/4

IR333/H0/L10

Features

- High reliability
- High radiant intensity
- Peak wavelength λ p=940nm
- 2.54mm Lead spacing
- Low forward voltage
- Pb free
- The product itself will remain within RoHS compliant version.

Descriptions

- EVERLIGHT'S Infrared Emitting Diode(IR333/H0/L10) is a high intensity diode , molded in a blue transparent plastic package.
- The device is spectrally matched with phototransistor , photodiode and infrared receiver module.

Applications

- Free air transmission system
- Infrared remote control units with high power requirement
- Smoke detector
- Infrared applied system

Device Selection Guide

LED Part No.	Chip Material	Lens Color
IR	GaAlAs	Blue

Package Dimensions

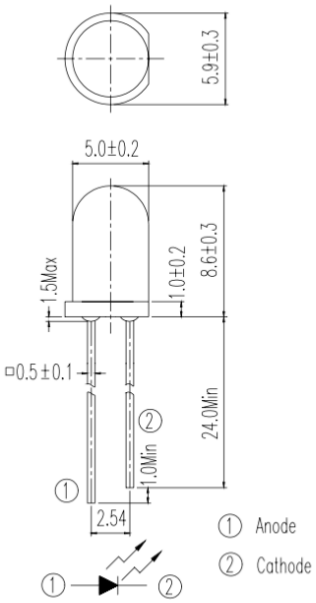

Notes: 1.All dimensions are in millimeters
2.Tolerances unless dimensions ±0.25mm

Absolute Maximum Ratings (Ta=25℃)

Parameter	Symbol	Rating	Units
Continuous Forward Current	I_F	100	mA
Peak Forward Current	I_{FP}	1.0	A
Reverse Voltage	V_R	5	V
Operating Temperature	T_{opr}	-40 ~ +85	℃
Storage Temperature	T_{stg}	-40 ~ +85	℃
Soldering Temperature	T_{sol}	260	℃
Power Dissipation at(or below) 25℃ Free Air Temperature	P_d	150	mW

Notes: *1:I_{FP} Conditions--Pulse Width≦100 μs and Duty≦1%.
*2:Soldering time≦5 seconds.

Electro-Optical Characteristics (Ta=25℃)

Parameter	Symbol	Condition	Min.	Typ.	Max.	Units
Radiant Intensity	Ee	I_F=20mA	11	12	--	mW/sr
		I_F=100mA Pulse Width≦100 μs ,Duty≦1%	--	45	--	
		I_F=1A Pulse Width≦100 μs ,Duty≦1%.	--	400	--	
Peak Wavelength	λp	I_F=20mA	--	940	--	nm
Spectral Bandwidth	Δλ	I_F=20mA	--	45	--	nm
Forward Voltage	V_F	I_F=20mA		1.2	1.5	V
		I_F=100mA Pulse Width≦100 μs ,Duty≦1%	--	1.4	1.8	
		I_F=1A Pulse Width≦100 μs ,Duty≦1%.	--	2.6	4.0	
Reverse Current	I_R	V_R=5V	--	--	10	μA
View Angle	2θ 1/2	I_F=20mA	--	40	--	deg

Typical Electro-Optical Characteristics Curves

Fig.1 Forward Current vs. Ambient Temperature

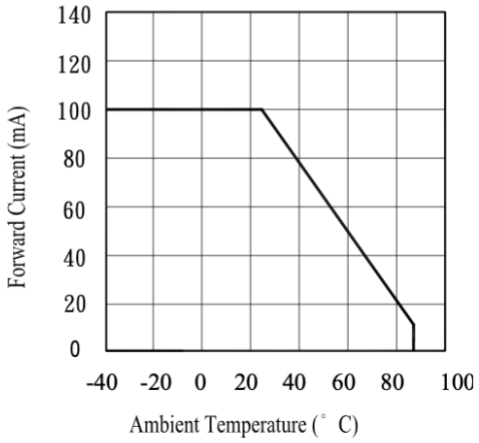

Fig.2 Spectral Distribution

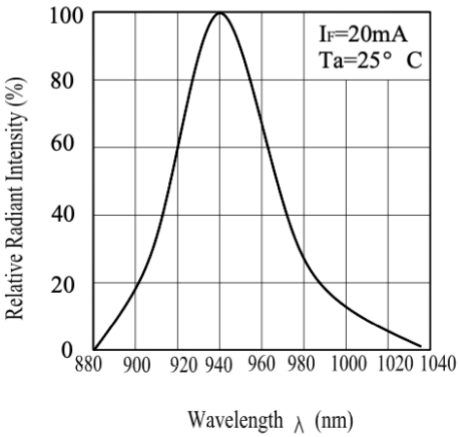

Fig.3 Peak Emission Wavelength Ambient Temperature

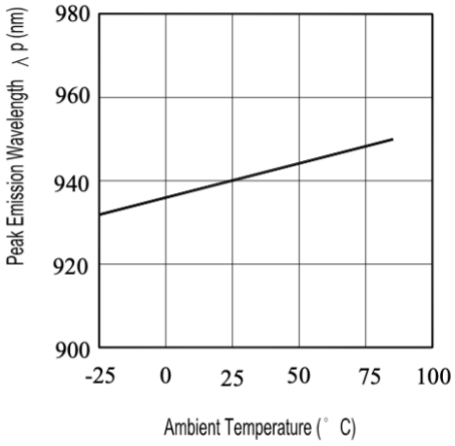

Fig.4 Forward Current vs. Forward Voltage

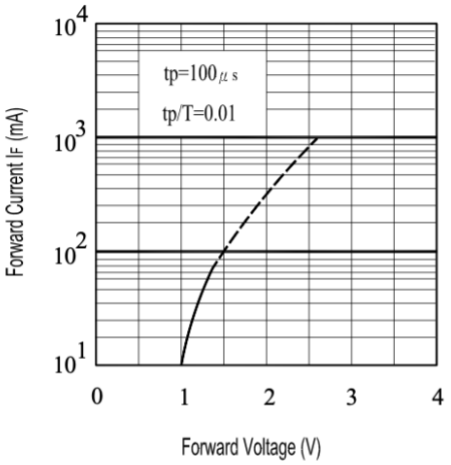

Typical Electro-Optical Characteristics Curves

Fig.5 Relative Intensity vs. Forward Current

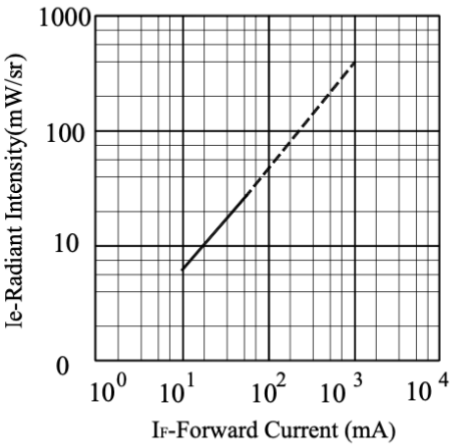

Fig.6 Relative Radiant Intensity vs. Angular Displacement

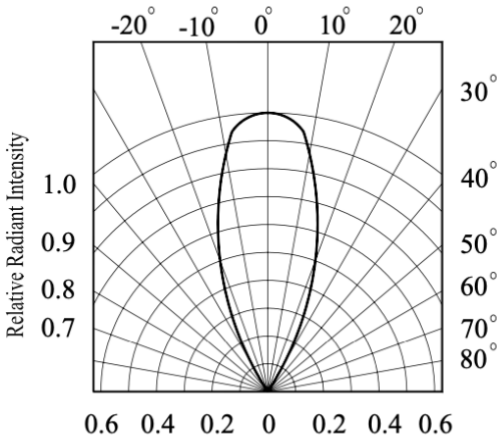

Fig.7 Relative Intensity vs. Ambient Temperature(°C)

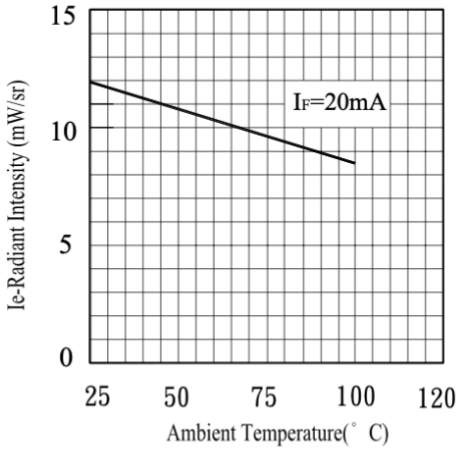

Fig.8 Forward Voltage vs. Ambient Temperature(°C)

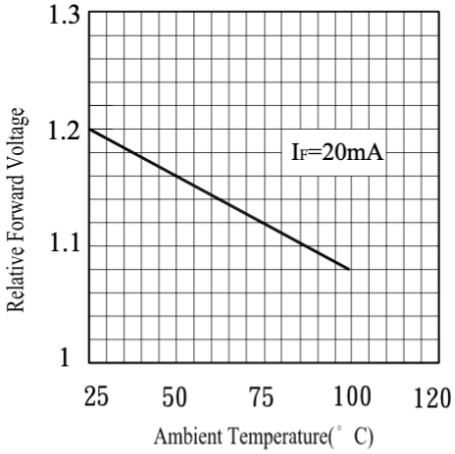

Reliability Test Item And Condition

The reliability of products shall be satisfied with items listed below.

Confidence level：90%

LTPD：10%

NO.	Item	Test Conditions	Test Hours/ Cycles	Sample Sizes	Failure Judgement Criteria	Ac/Re
1	Solder Heat	TEMP.：260℃±5℃	10secs	22pcs	$I_R \geqq U \times 2$ $Ee \leqq L \times 0.8$ $V_F \geqq U \times 1.2$ U：Upper Specification Limit L：Lower Specification Limit	0/1
2	Temperature Cycle	H：+100℃ 15mins ↕ 5mins L：-40℃ 15mins	300Cycles	22pcs		0/1
3	Thermal Shock	H：+100℃ 5mins ↕ 10secs L：-10℃ 5mins	300Cycles	22pcs		0/1
4	High Temperature Storage	TEMP.：+100℃	1000hrs	22pcs		0/1
5	Low Temperature Storage	TEMP.：-40℃	1000hrs	22pcs		0/1
6	DC Operating Life	I_F=20mA	1000hrs	22pcs		0/1
7	High Temperature/ High Humidity	85℃ / 85% R.H	1000hrs	22pcs		0/1

Packing Quantity Specification

1.500PCS/1Bag，5Bags/1Box

2.10Boxes/1Carton

Label Form Specification

CPN: Customer's Production Number
P/N : Production Number
QTY: Packing Quantity
AT: Ranks
HUE: Peak Wavelength
REF: Reference
LOT No: Lot Number
MADE IN TAIWAN: Production Place

Notes

1. Above specification may be changed without notice. EVERLIGHT will reserve authority on material change for above specification.
2. When using this product, please observe the absolute maximum ratings and the instructions for using outlined in these specification sheets. EVERLIGHT assumes no responsibility for any damage resulting from use of the product which does not comply with the absolute maximum ratings and the instructions included in these specification sheets.
3. These specification sheets include materials protected under copyright of EVERLIGHT corporation. Please don't reproduce or cause anyone to reproduce them without EVERLIGHT's consent.

EVERLIGHT ELECTRONICS CO., LTD.
Office: No 25, Lane 76, Sec 3, Chung Yang Rd, Tucheng, Taipei 236, Taiwan, R.O.C
Tel: 886-2-2267-2000, 2267-9936
Fax: 886-2267-6244, 2267-6189, 2267-6306
http:\\www.everlight.com

LPT 80 A

Radial Sidelooker

Silicon NPN Phototransistor

Applications

- Electronic Equipment
- Highbay Industrial
- Industrial Automation (Machine Controls, Light Barriers, Vision Controls)
- White Goods

Features:

- Package: clear epoxy
- ESD: 2 kV acc. to ANSI/ESDA/JEDEC JS-001 (HBM, Class 2)
- Spectral range of sensitivity: (typ) 450 ... 1100 nm
- High photosensitivity
- Same package as IR emitter IRL 81 A

Ordering Information

Type	Photocurrent [1] V_{CE} = 5 V; λ = 950 nm; E_e = 0.5 mW/cm² I_{PCE}	Photocurrent [2] typ. V_{CE} = 5 V; λ = 950 nm; E_e = 0.5 mW/cm² I_{PCE}	Ordering Code
LPT 80A	≥ 280 µA	700 µA	Q68000A7852

Maximum Ratings

T_A = 25 °C

Parameter	Symbol		Values
Operating temperature	T_{op}	min. max.	-40 °C 100 °C
Storage temperature	T_{stg}	min. max.	-40 °C 100 °C
Collector-emitter voltage	V_{CE}	max.	30 V
Collector current	I_C	max.	50 mA
Collector surge current $\tau \leq 10$ µs	I_{CS}	max.	100 mA
Emitter-collector voltage	V_{EC}	max.	7 V
Total power dissipation	P_{tot}	max.	100 mW
ESD withstand voltage acc. to ANSI/ESDA/JEDEC JS-001 (HBM, Class 2)	V_{ESD}	max.	2 kV

Characteristics

T_A = 25 °C

Parameter	Symbol		Values
Wavelength of max sensitivity	$\lambda_{S\,max}$	typ.	880 nm
Spectral range of sensitivity	$\lambda_{10\%}$	typ.	450 ... 1100 nm
Dimensions of chip area	L x W	typ.	0.55 x 0.55 mm x mm
Radiant sensitive area	A	typ.	0.11 mm²
Half angle	φ	typ.	35 °
Photocurrent V_{CE} = 5 V; Std. Light A; E_v = 1000 lx	I_{PCE}	typ.	3200 µA
Dark current V_{CE} = 20 V; E = 0	I_{CE0}	typ. max.	1 nA 50 nA
Rise time I_C = 1 mA; λ = 0 nm; V_{CC} = 5 V; R_L = 1 kΩ	t_r	typ.	10 µs
Fall time I_C = 1 mA; λ = 0 nm; V_{CC} = 5 V; R_L = 1 kΩ	t_f	typ.	10 µs
Collector-emitter saturation voltage [3)] Threefold saturated	V_{CEsat}	typ.	150 mV
Capacitance V_{CE} = 0 V; f = 1 MHz; E = 0	C_{CE}	typ.	7.5 pF
Thermal resistance junction ambient real	R_{thJA}	max.	750 K / W

Relative Spectral Sensitivity 4), 5)

$S_{rel} = f(\lambda)$

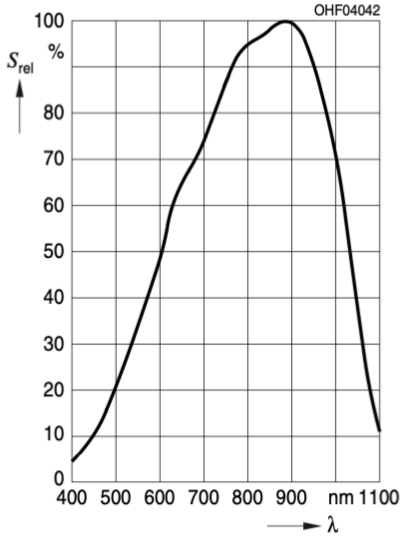

Directional Characteristics 4), 5)

$S_{rel} = f(\varphi)$

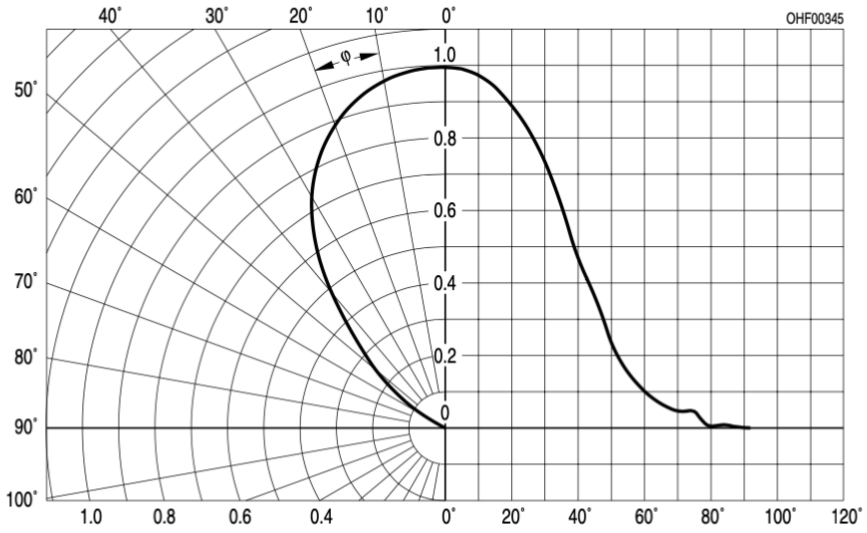

Photocurrent [4), 5)]

$I_{PCE} = f(E_e)$; $V_{CE} = 5$ V

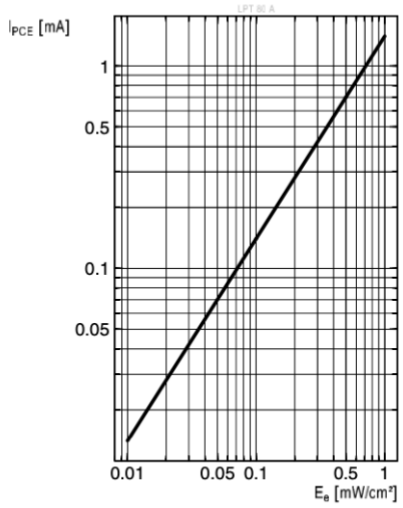

Dark Current [4), 5)]

$I_{CE0} = f(V_{CE})$; E = 0

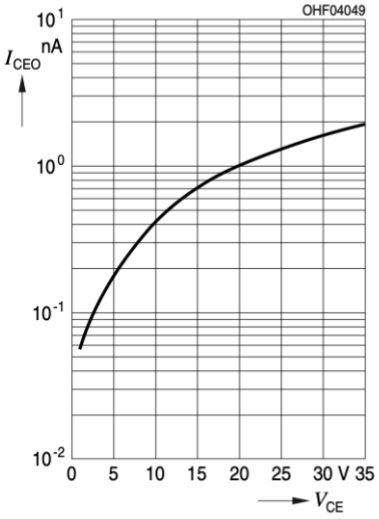

Collector-Emitter Capacitance [4), 5)]

$C_{CE} = f(V_{CE})$; f = 1 MHz; E = 0

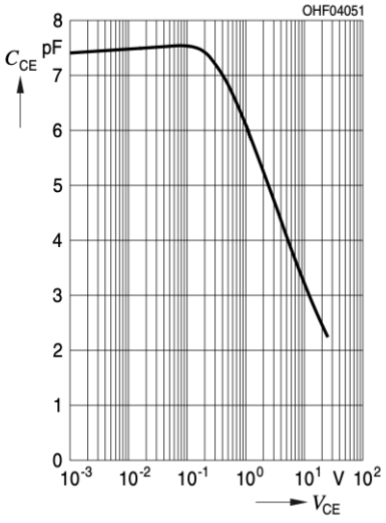

Dark Current [4)]

$I_{CE0} = f(T_A)$; $V_{CE} = 5$ V; $E_e = 0$ mW/cm²

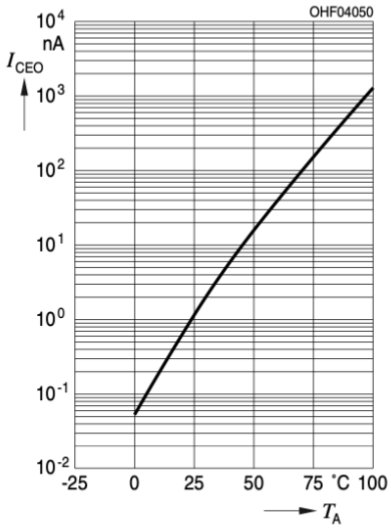

Photocurrent [4)]

$I_{PCE,rel} = f(T_A)$; $V_{CE} = 5$ V; $E_v = 1000$ lx

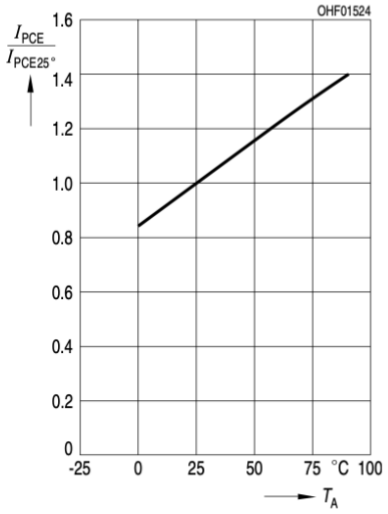

Power Consumption

$P_{tot} = f(T_A)$

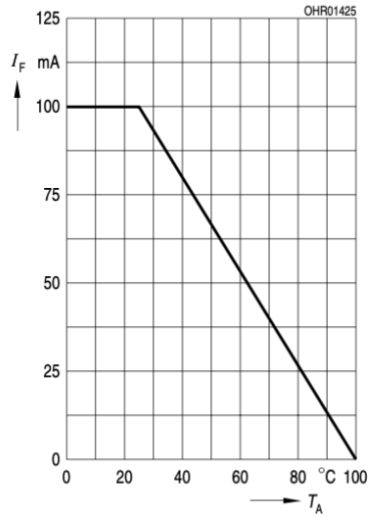

Dimensional Drawing [6)]

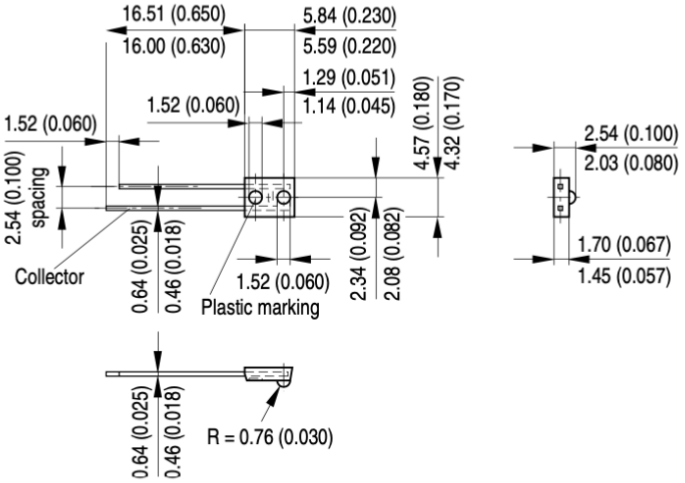

Approx. weight 0.2 g

GEOY6391

Further Information:

Approximate Weight: 157.0 mg

Package marking: Collector

Recommended Solder Pad [6)]

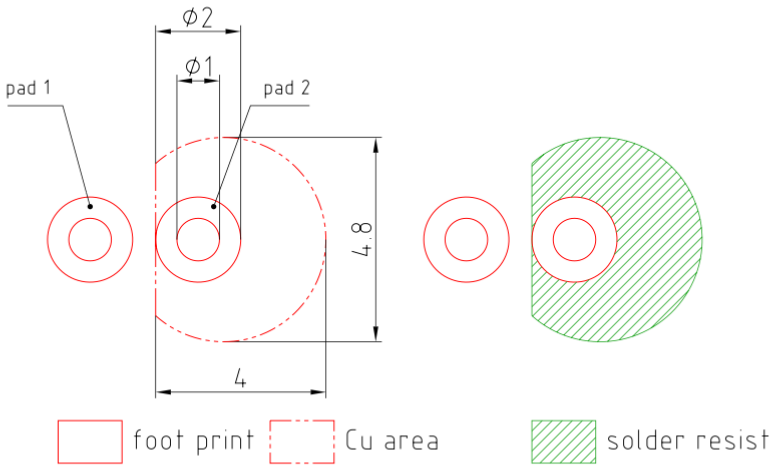

E062.3010.188-01

TTW Soldering

IEC-61760-1 TTW

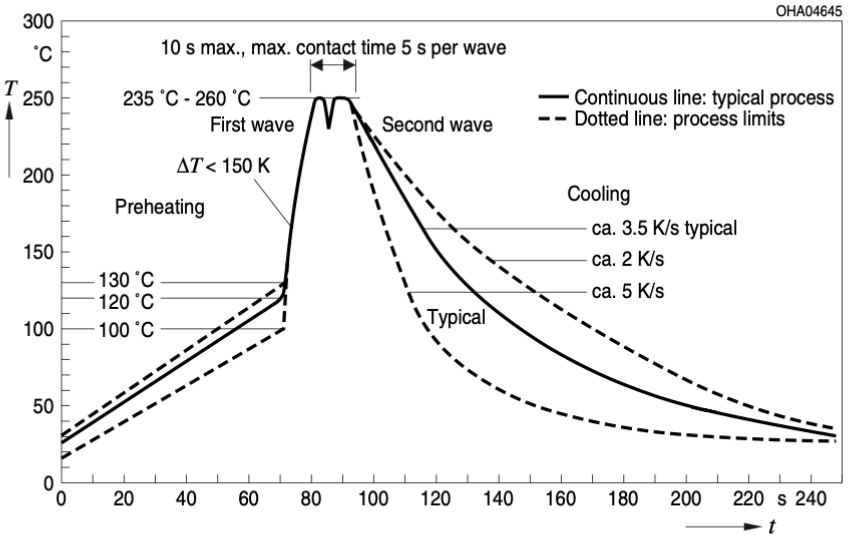

XICON

Metal Oxide Power Resistors (RoHS Compliant) MO-RC Series

■ FEATURES

- Temperature Range: -55°C ~ +235°C (derated over 70°C)
- ±5% tolerance
- Excellent flame retardant coating
- Stable performance in diverse environments
- High purity ceramic core
- Other values may be available on request

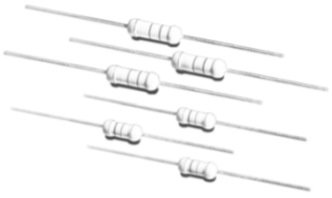

LEAD-FREE

Environmental Commitment

■ DERATING CURVE

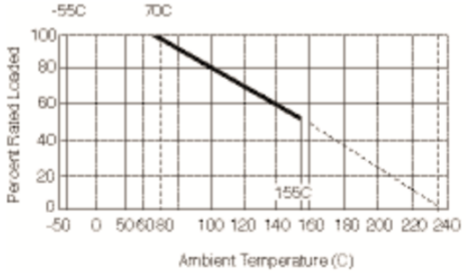

Suffix Code:	Package:
(blank)	Bulk
REEL	Tape and Reel

■ PART NUMBERING SYSTEM

2	8	1	-	1	0	K	/	R	E	E	L	-	R	C
Series				Value				Suffix					Suffix (RoHS Compliant)	

■ SERIES, SIZE, WATTAGE, RANGE OF VALUES, VOLTAGE, AND DIMENSIONS

Series	Case Size	Watts (W)	Standard Range of Values	Voltage (V) (max.) @ 70°C			Dimensions (mm)			
				Working	Overload	Withstanding	L (max.)	D (max.)	H ±3	d, ±.05
281	Small	1	0.1 ~ 1.0M	350	600	350	10	3.5	28	0.54
282	Small	2	0.1 ~ 1.0M	350	600	350	12	5	25	0.7
283	Small	3	0.1 ~ 1.0M	350	600	350	16	5.5	28	0.7
286	Small	5	0.22 ~ 560K	500	800	500	25	8	38	0.75
261	Standard	1	0.1 ~ 1.0M	350	600	350	12	5	25	0.7
262	Standard	2	0.1 ~ 1.0M	350	600	350	16	5.5	28	0.7

■ STANDARD STOCKED VALUES (Ω)

0.47	0.82	1.6	3.3	6.2	12	24	47	91	180	360	680	1.3K	2.7K	5.1K	10K	20K	39K	75K	150K	300K	560K
0.5	0.91	1.8	3.6	6.8	13	27	51	100	200	390	750	1.5K	3.0K	5.6K	11K	22K	43K	82K	160K	330K	620K
0.51	1.0	2.0	3.9	7.5	15	30	56	110	220	430	820	1.6K	3.3K	6.2K	12K	24K	47K	91K	180K	360K	680K
0.56	1.1	2.2	4.3	8.2	16	33	62	120	240	470	910	1.8K	3.6K	6.8K	13K	27K	51K	100K	200K	390K	750K
0.62	1.2	2.4	4.7	9.1	18	36	68	130	270	510	1.0K	2.0K	3.9K	7.5K	15K	30K	56K	110K	220K	430K	820K
0.68	1.3	2.7	5.1	10	20	39	75	150	300	560	1.1K	2.2K	4.3K	8.2K	16K	33K	62K	120K	240K	470K	910K
0.75	1.5	3.0	5.6	11	22	43	82	160	330	620	1.2K	2.4K	4.7K	9.1K	18K	36K	68K	130K	270K	510K	1.0M

A.2 The Hardware

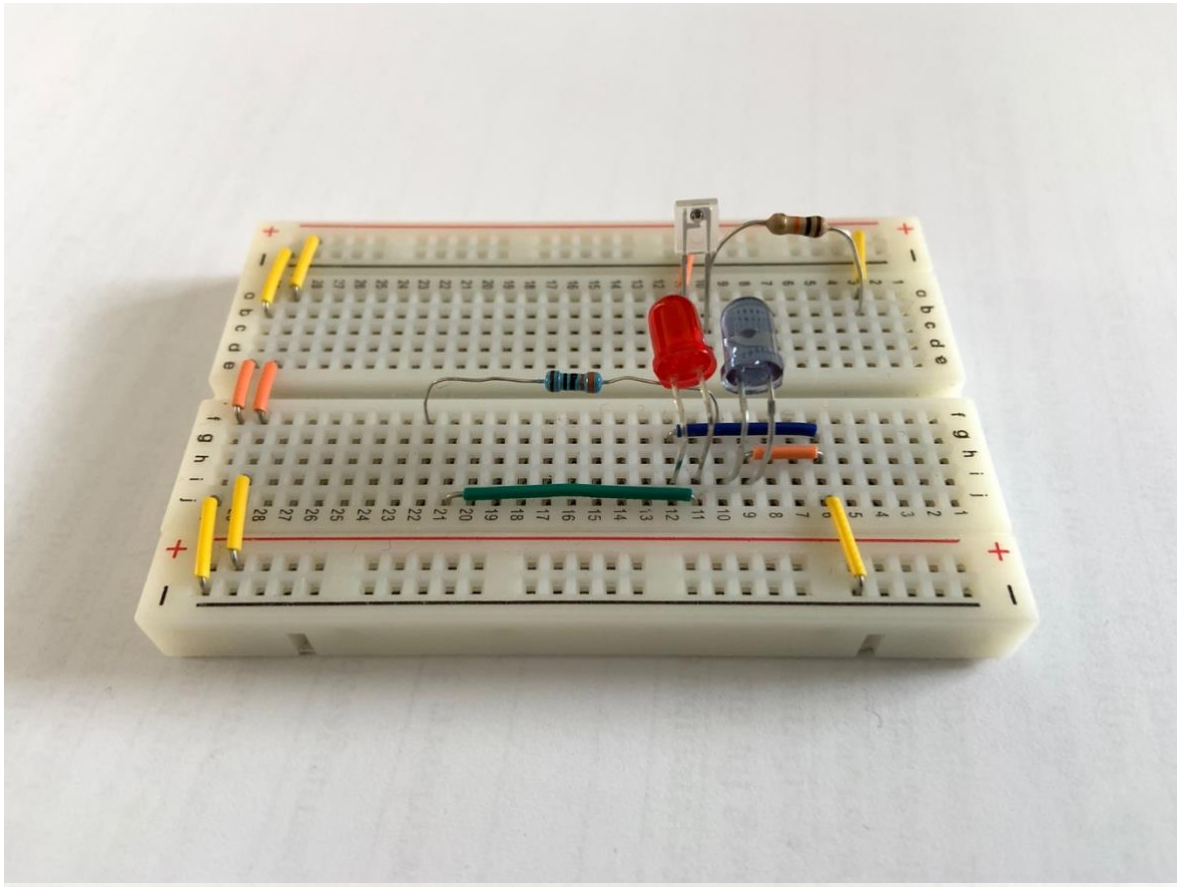

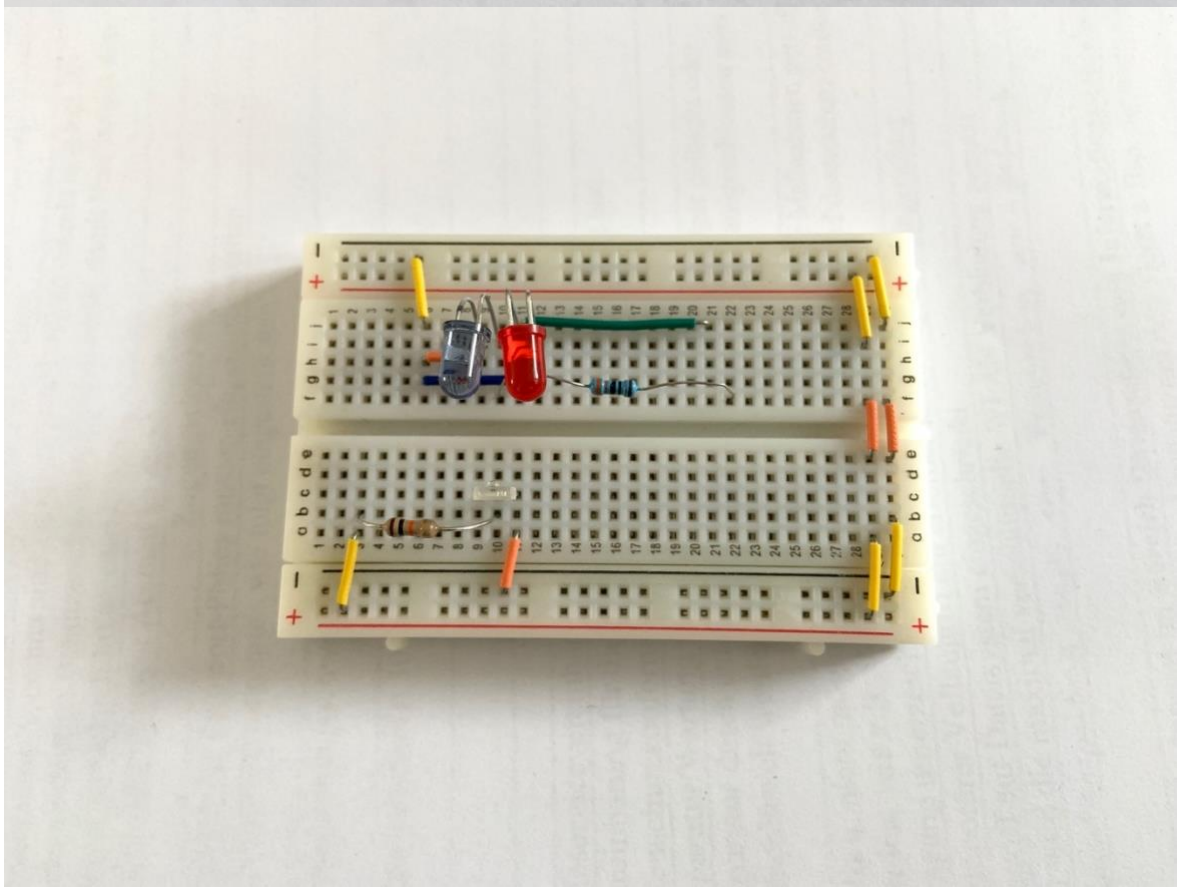

A.3 The sketch

Final_code §

```
#include <Wire.h>

#define maxperiod_siz 80 // max number of samples in a period
#define measures 10      // number of periods stored
#define samp_siz 4       // number of samples for average
#define rise_threshold 3 // number of rising measures to determine a peak

int T = 20;
int sensorPin = A0;
int REDLed = 3;
int IRLed = 4;

byte sym[3][8] = {
 {
  B00000,
  B01010,
  B11111,
  B11111,
  B01110,
  B00100,
  B00000,
  B00000
},{
  B00000,
  B00000,
  B00000,
  B11000,
  B00100,
  B01000,
  B10000,
  B11100
},{
  B00000,
  B00100,
  B01010,
  B00010,
```

```
  B00100,
  B00100,
  B00000,
  B00100
}
};

void setup() {
  // put your setup code here, to run once:
  Serial.begin(9600);
  Serial.flush();
  pinMode(sensorPin,INPUT_PULLUP);
  pinMode(REDLed,OUTPUT);
  pinMode(IRLed,OUTPUT);

  digitalWrite(REDLed,LOW);
  digitalWrite(IRLed,LOW);

}

void loop() {
  // put your main code here, to run repeatedly:

  bool finger_status = true;
  //
  float readsIR[samp_siz], sumIR,lastIR, reader, start;
  float readsRED[samp_siz], sumRED,lastRED;

//
  int period, samples;
  period=0; samples=0;
  int samplesCounter = 0;
  float readsIRMM[maxperiod_siz],readsREDMM[maxperiod_siz];
  int ptrMM =0;
  for (int i = 0; i < maxperiod_siz; i++) { readsIRMM[i] = 0;readsREDMM[i]=0;}
  float IRmax=0;
  float IRmin=0;
  float REDmax=0;
  float REDmin=0;
  double R=0;

  float measuresR[measures];
  int measuresPeriods[measures];
  int m = 0;
  for (int i = 0; i < measures; i++) { measuresPeriods[i]=0; measuresR[i]=0; }

  int ptr;

  float beforeIR;

  bool rising;
  int rise_count;
  int n;
  long int last_beat;
  for (int i = 0; i < samp_siz; i++) { readsIR[i] = 0; readsRED[i]=0; }
  sumIR = 0; sumRED=0;
  ptr = 0;

  while(1)
  {

    //
    // turn on IR LED
    digitalWrite(REDLed,LOW);
    digitalWrite(IRLed,HIGH);

    // calculate an average of the sensor
    // during a 20 ms (T) period (this will eliminate
    // the 50 Hz noise caused by electric light
    n = 0;
    start = millis();
    reader = 0.;
    do
    {
```

```
  reader += analogRead(sensorPin);
  n++;
}
while (millis() < start + T);
reader /= n;  // we got an average
// Add the newest measurement to an array
// and subtract the oldest measurement from the array
// to maintain a sum of last measurements
sumIR -= readsIR[ptr];
sumIR += reader;
readsIR[ptr] = reader;
lastIR = sumIR / samp_siz;

//
// TURN ON RED LED and do the same

digitalWrite(REDLed,HIGH);
digitalWrite(IRLed,LOW);

n = 0;
start = millis();
reader = 0.;
do
{
  reader += analogRead(sensorPin);
  n++;
}
while (millis() < start + T);
reader /= n;  // we got an average
// Add the newest measurement to an array
// and subtract the oldest measurement from the array
// to maintain a sum of last measurements
sumRED -= readsRED[ptr];
sumRED += reader;
readsRED[ptr] = reader;
lastRED = sumRED / samp_siz;
```

```
//
// R CALCULATION
// save all the samples of a period both for IR and for RED
readsIRMM[ptrMM]=lastIR;
readsREDMM[ptrMM]=lastRED;
ptrMM++;
ptrMM %= maxperiod_siz;
samplesCounter++;
//
// if I've saved all the samples of a period, look to find
// max and min values and calculate R parameter
if(samplesCounter>=samples){
  samplesCounter =0;
  IRmax = 0; IRmin=1023; REDmax = 0; REDmin=1023;
  for(int i=0;i<maxperiod_siz;i++) {
    if( readsIRMM[i]> IRmax) IRmax = readsIRMM[i];
    if( readsIRMM[i]>0 && readsIRMM[i]< IRmin ) IRmin = readsIRMM[i];
    readsIRMM[i] =0;
    if( readsREDMM[i]> REDmax) REDmax = readsREDMM[i];
    if( readsREDMM[i]>0 && readsREDMM[i]< REDmin ) REDmin = readsREDMM[i];
    readsREDMM[i] =0;
  }
  R =  ( (REDmax-REDmin) / REDmin) / ( (IRmax-IRmin) / IRmin ) ;
  Serial.println("R= " + String(R));

}

// check that the finger is placed inside
// the sensor. If the finger is missing
// RED curve is under the IR.
//
if (lastRED < lastIR) {
  if(finger_status==true) {
    finger_status = false;
    Serial.print("No Finger?");
   }
```

```
} else {
  if(finger_status==false) {
    finger_status = true;
  }
}
float avR = 0;
int avBPM=0;

if (finger_status==true){

   // lastIR holds the average of the values in the array
   // check for a rising curve (= a heart beat)
   if (lastIR > beforeIR)
   {

     rise_count++;  // count the number of samples that are rising
     if (!rising && rise_count > rise_threshold)
     {
        rising = true;

        measuresR[m] = R;
        measuresPeriods[m] = millis() - last_beat;
        last_beat = millis();
        int period = 0;
        for(int i =0; i<measures; i++) period += measuresPeriods[i];

        // calculate average period and number of samples
        // to store to find min and max values
        period = period / measures;
        samples = period / (2*T);

        int avPeriod = 0;
        int c = 0;

        // c stores the number of good measures (not floating more than 10%),
        // in the last 10 peaks
        for(int i =1; i<measures; i++) {
          if ( (measuresPeriods[i] <  measuresPeriods[i-1] * 1.1)  &&
                (measuresPeriods[i] >  measuresPeriods[i-1] / 1.1)  ) {

             c++;
             avPeriod += measuresPeriods[i];
             avR += measuresR[i];

          }
        }

        m++;
        m %= measures;
        Serial.println("c= " + String(c)+" ");

        // bpm and R shown are calculated as the
        // average of at least 5 good peaks
        avBPM = 60000 / ( avPeriod / c) ;
        avR = avR / c ;

        // if there are at last 5 measures
        if(c > 4) {

          //
          // SATURTION IS A FUNCTION OF R (calibration)
          // Y = k*x + m
          // k and m are calculated with another oximeter
          int SpO2 = -19 * R + 112;

          if(avBPM > 40 && avBPM <220) Serial.print("avBPM= " + String(avBPM)+" "); else Serial.println("---");

          if(SpO2 > 70 && SpO2 <150) Serial.print("Sp02= " + String(SpO2) + "%"); else Serial.println("---%");

        }
     }
   }
   else
   {
```

```
        // Ok, the curve is falling
        rising = false;
        rise_count = 0;
        //Serial.println(" ");
      }

      // to compare it with the new value and find peaks
      beforeIR = lastIR;


  } // finger is inside

   // PLOT everything
   /*
   Serial.print(lastIR);
   Serial.print(",");
   Serial.print(lastRED);


   Serial.print(",");
   Serial.print(R);
   Serial.print(",");
   Serial.print(IRmax);
   Serial.print(",");
   Serial.print(IRmin);
   Serial.print(",");
   Serial.print(REDmax);
   Serial.print(",");
   Serial.print(REDmin);
   Serial.print(",");
   Serial.print(avR);
   Serial.print(",");
   Serial.print(avBPM); */
   Serial.println();


  // handle the arrays
  ptr++;
  ptr %= samp_siz;


 } // loop while 1
}
```

A.4 Individual results of data collection

Participant one

Measuring cycle	Time	R-value prototype	SpO2 prototype	SpO2 Sanitas	BPM Prototype	BPM Sanitas
	21:53:08	0,05	111 %	-	78	-
	21:53:11	0,02	111 %	-	79	-
	21:53:12	0,04	111 %	98 %	79	79
	21:53:13	0,02	111 %	98 %	79	79
1.	21:53:13	0,11	109 %	98 %	79	79
	21:53:14	0,03	111 %	98 %	79	79
	21:53:15	0,12	109 %	98 %	78	79
	21:53:16	0,08	110 %	98 %	78	79
	21:53:16	0,86	95 %	98 %	78	79
	21:53:18	0,71	98 %	98 %	78	79
	21:53:19	0,12	100 %	98 %	78	80
	21:53:19	0,93	99 %	98 %	78	80
	21:53:21	0,6	107 %	98 %	77	79
	21:53:22	0,67	111 %	98 %	77	79
2.	21:53:54	0,22	111 %	98 %	77	72
	21:53:55	0,02	111 %	98 %	77	72
	21:53:55	0,03	109 %	98 %	77	73
	21:53:57	0,05	109 %	98 %	77	74
	21:53:57	0,11	111 %	98 %	76	74
	21:53:58	0,13	110 %	98 %	77	74
	21:53:59	0,05	111 %	98 %	76	74
	21:54:00	0,06	110 %	98 %	77	74
	21:54:00	0,05	111 %	98 %	77	74
	21:54:01	0,13	109 %	98 %	76	75
3.	21:54:02	0,04	111 %	98 %	75	77
	21:54:03	0,08	110 %	98 %	75	78
	21:54:16	0,06	110 %	98 %	78	77
	21:54:18	0,14	109 %	98 %	73	77
	21:54:18	0,08	110 %	98 %	73	77
	21:54:19	0,03	111 %	98 %	73	76
	22:54:20	0,07	110 %	98 %	73	75
	21:54:21	0,07	110 %	98 %	74	75
	21:54:22	0,16	108 %	98 %	75	75
	21:54:22	0,03	111 %	98 %	75	75
4.	21:54:23	0,04	111 %	98 %	75	74
	21:54:24	0,1	110 %	98 %	74	73
	21:54:25	0,14	109 %	98 %	75	73
	21:54:25	0,05	111 %	98 %	76	73
	21:54:26	0,03	111 %	98 %	86	73
	21:54:27	0,03	111 %	98 %	86	73
	21:54:27	0,09	110 %	98 %	86	73
	21:54:29	0,1	110 %	98 %	85	73
	21:54:29	0,02	111 %	98 %	84	73
	21:54:30	0,04	111 %	98 %	85	74
5.	21:54:31	0,05	111 %	98 %	85	75
	21:54:41	0,02	111 %	98 %	77	76
	21:54:48	0,08	110 %	98 %	77	76
	21:54:50	0,02	111 %	98 %	71	76
	21:54:51	0,03	111 %	98 %	71	76
	21:54:52	0,06	110 %	98 %	72	76
	21:54:53	0,06	110 %	98 %	71	76
	21:54:54	0,05	111 %	98 %	71	76
	21:54:55	0,03	111 %	98 %	72	76
	21:54:55	0,1	110 %	98 %	73	76
6.	21:54:56	0,05	111 %	98 %	73	76
	21:54:57	0,05	111 %	98 %	75	76
	21:54:58	0,03	111 %	98 %	76	76
	21:54:59	0,05	111 %	98 %	76	76
	21:54:59	0,03	111 %	98 %	76	76
	21:55:00	0,06	110 %	98 %	76	76
	21:55:01	0,43	103 %	98 %	76	76
	21:55:02	0,08	110 %	98 %	76	76
	21:55:03	0,05	111 %	98 %	76	76

Participant two

Measuring cycle	Time	R-value prototype	SpO2 prototype	SpO2 Sanitas	BPM Prototype	BPM Sanitas
	21:47:28	0.05	111 %	-	73	-
	21:47:29	0.04	111 %	-	73	-
	21:47:30	0.06	110 %	-	72	-
	21:47:31	0.03	111 %	-	73	-
1.	21:47:32	0.03	111 %	-	72	-
	21:47:32	0.04	111 %	-	73	-
	21:47:33	0.04	111 %	-	73	-
	21:47:34	0.07	110 %	-	74	-
	21:47:35	0.04	111 %	98 %	74	78
	21:47:36	0.04	111 %	98 %	74	78
	21:47:37	0.03	111 %	98 %	74	78
	21:47:37	0.03	111 %	98 %	74	78
	21:47:47	0.10	110 %	98 %	66	70
	21:47:48	0.08	110 %	98 %	67	69
2.	21:47:49	0.11	109 %	98 %	67	69
	21:47:50	0.11	109 %	98 %	67	69
	21:47:50	0.17	108 %	98 %	68	69
	21:47:51	0.09	110 %	98 %	68	69
	21:47:52	0.08	110 %	98 %	70	68
	21:47:53	0.09	110 %	98 %	70	68
	21:47:54	0.08	110 %	98 %	70	68
	21:47:55	0.05	111 %	98 %	69	68
	21:47:55	0.03	111 %	98 %	69	68
	21:47:56	0.05	111 %	98 %	69	68
3.	21:47:57	0.05	111 %	98 %	69	68
	21:47:59	0.02	111 %	98 %	64	67
	21:48:01	0.04	111 %	98 %	64	67
	21:48:02	0.02	111 %	98 %	63	67
	21:48:03	0.06	110 %	98 %	64	67
	21:48:04	0.08	110 %	98 %	64	67
	21:48:04	0.09	110 %	98 %	66	67
	21:48:05	0.07	110 %	98 %	69	67
	21:48:09	0.03	111 %	98 %	69	67
	21:48:10	0.08	110 %	98 %	67	67
4.	21:48:11	0.04	111 %	98 %	66	67
	21:48:14	0.07	110 %	98 %	62	66
	21:48:15	0.12	109 %	98 %	61	67
	21:48:16	0.11	109 %	98 %	61	67
	21:48:17	0.09	110 %	98 %	61	67
	21:48:18	0.11	109 %	98 %	63	67
	21:48:19	0.15	109 %	98 %	65	68
	21:48:20	0.13	109 %	98 %	66	68
	21:48:21	0.11	109 %	98 %	66	68
	21:48:22	0.08	110 %	98 %	67	68
5.	21:48:23	0.11	109 %	98 %	67	68
	21:48:24	0.07	110 %	98 %	67	68
	21:48:25	0.13	109 %	98 %	68	68
	21:48:26	0.16	108 %	98 %	68	68
	21:48:27	0.07	110 %	98 %	67	68
	21:48:28	0.09	110 %	98 %	67	68
	21:48:29	0.12	109 %	98 %	67	69
	21:48:30	0.10	110 %	98 %	67	68
	21:48:30	0.13	109 %	98 %	67	68
	21:48:31	0.09	110 %	98 %	68	68
6.	21:48:32	0.12	109 %	98 %	68	68
	21:48:33	0.18	108 %	98 %	67	68
	21:48:34	0.11	109 %	98 %	67	68
	21:48:35	0.09	110 %	98 %	67	68
	21:48:36	0.10	110 %	98 %	67	68
	21:48:37	0.10	110 %	98 %	67	68
	21:48:37	0.11	109 %	98 %	67	68
	21:48:38	0.12	109 %	98 %	67	68
	21:48:39	0.12	109 %	98 %	67	68
	21:48:40	0.12	109 %	98 %	67	68

7.	21:48:41	0.13	109 %	98 %	67	67
	21:48:42	0.13	109 %	98 %	70	67
	21:48:43	0.09	110 %	98 %	70	67
	21:48:44	0.11	109 %	98 %	70	66
	21:48:45	0.11	109 %	98 %	71	66
	21:48:46	0.10	110 %	98 %	70	66
	21:48:47	0.07	110 %	98 %	69	66
	21:48:48	0.11	109 %	98 %	68	66
	21:48:49	0.14	109 %	98 %	68	66
	21:48:50	0.12	109 %	98 %	68	66
8.	21:48:51	0.10	110 %	98 %	69	66
	21:48:52	0.09	110 %	98 %	69	66
	21:48:53	0.10	110 %	98 %	69	66
	21:48:54	0.08	110 %	98 %	71	66
	21:48:54	0.11	109 %	98 %	71	66
	21:48:55	0.07	110 %	98 %	71	66
	21:48:56	0.08	110 %	98 %	71	66
	21:48:57	0.09	110 %	98 %	71	67
	21:48:58	0.08	110 %	98 %	71	67
	21:48:59	0.05	111 %	98 %	69	67
9.	21:49:00	0.04	111 %	98 %	69	68
	21:49:01	0.06	110 %	98 %	69	68
	21:49:01	0.08	110 %	98 %	69	68
	21:49:02	0.06	110 %	98 %	69	68
	21:49:03	0.07	110 %	98 %	68	68
	21:49:04	0.08	110 %	98 %	68	68
	21:49:05	0.10	110 %	98 %	70	68
	21:49:06	0.08	110 %	98 %	69	69
	21:49:07	0.11	109 %	98 %	67	69
	21:49:08	0.10	110 %	98 %	66	69
10.	21:49:10	0.09	110 %	98 %	66	68
	21:49:11	0.11	109 %	98 %	66	68
	21:49:11	0.13	109 %	98 %	66	68
	21:49:12	0.13	109 %	98 %	66	68
	21:49:13	0.14	109 %	98 %	66	68
	21:49:14	0.09	110 %	98 %	66	68
	21:49:15	0.12	109 %	98 %	65	67
	21:49:16	0.13	109 %	98 %	66	67
	21:49:17	0.10	110 %	98 %	67	66
	21:49:18	0.11	109 %	98 %	67	67
11.	21:49:19	0.09	110 %	98 %	67	67
	21:49:20	0.08	110 %	98 %	67	67
	21:49:21	0.12	109 %	98 %	68	67
	21:49:22	0.10	110 %	98 %	67	65
	21:49:23	0.10	110 %	98 %	66	65
	21:49:24	0.11	109 %	98 %	67	65
	21:49:25	0.10	110 %	98 %	67	65
	21:49:26	0.11	109 %	98 %	67	65
	21:49:27	0.09	110 %	98 %	67	65
	21:49:28	0.10	110 %	98 %	66	65
12.	21:49:29	0.12	109 %	98 %	67	66
	21:49:30	0.11	109 %	98 %	66	66
	21:49:31	0.13	109 %	98 %	66	66
	21:49:32	0.14	109 %	98 %	67	66
	21:49:33	0.12	109 %	98 %	67	66
	21:49:34	0.11	109 %	98 %	67	66
	21:49:35	0.12	109 %	98 %	67	66
	21:49:36	0.10	110 %	98 %	67	66
	21:49:37	0.09	110 %	98 %	67	66
	21:49:38	0.08	110 %	98 %	67	66

13.	21:49:39	0.10	110 %	98 %	68	66
	21:49:40	0.06	110 %	98 %	68	66
	21:49:41	0.06	110 %	98 %	69	66
	21:49:42	0.08	110 %	98 %	69	66
	21:49:43	0.05	111 %	98 %	69	66
	21:49:44	0.04	111 %	98 %	69	66
	21:49:45	0.04	111 %	98 %	69	66
	21:49:46	0.05	111 %	98 %	70	66
	21:49:47	0.02	111 %	98 %	70	67
	21:49:48	0.04	111 %	98 %	70	67
14.	21:49:49	0.04	111 %	98 %	70	67
	21:49:50	0.04	111 %	98 %	70	67
	21:49:51	0.03	111 %	98 %	69	67
	21:49:52	0.03	111 %	98 %	69	67
	21:49:53	0.04	111 %	98 %	69	67
	21:49:54	0.03	111 %	98 %	69	67
	21:49:55	0.02	111 %	98 %	69	67
	21:49:56	0.03	111 %	98 %	69	67
	21:49:57	0.06	110 %	98 %	69	67
	21:49:58	0.03	111 %	98 %	69	70
15.	21:49:59	0.05	111 %	98 %	70	70
	21:50:00	0.07	110 %	98 %	68	70
	21:50:01	0.05	111 %	98 %	69	70
	21:50:02	0.04	111 %	98 %	69	70
	21:50:03	0.06	110 %	98 %	68	70
	21:50:04	0.03	111 %	98 %	68	70
	21:50:05	0.03	111 %	98 %	67	70
	21:50:06	0.05	111 %	98 %	67	70
	21:50:07	0.03	111 %	98 %	65	69
	21:50:08	0.06	110 %	98 %	66	69
16.	21:50:09	0.06	110 %	98 %	66	69
	21:50:10	0.05	111 %	98 %	66	69
	21:50:11	0.05	111 %	98 %	66	68
	21:50:12	0.05	111 %	98 %	67	68
	21:50:13	0.04	111 %	98 %	67	67
	21:50:14	0.03	111 %	98 %	66	67
	21:50:15	0.04	111 %	98 %	66	67
	21:50:16	0.02	111 %	98 %	66	67
	21:50:17	0.03	111 %	98 %	66	67
	21:50:18	0.03	111 %	98 %	66	67
17.	21:50:19	0.03	111 %	98 %	66	67
	21:50:20	0.02	111 %	98 %	66	67
	21:50:21	0.05	111 %	98 %	66	66
	21:50:27	0.06	110 %	98 %	66	65
	21:50:28	0.06	110 %	98 %	66	65
	21:50:29	0.04	111 %	98 %	66	66
	21:50:30	0.07	110 %	98 %	65	66
	21:50:31	0.04	111 %	98 %	65	66
	21:50:32	0.03	111 %	98 %	65	66
	21:50:33	0.05	111 %	98 %	65	66
18.	21:50:34	0.07	110 %	98 %	66	65
	21:50:35	0.02	111 %	98 %	66	65
	21:50:36	0.06	110 %	98 %	66	65
	21:50:37	0.07	110 %	98 %	66	65
	21:50:38	0.02	111 %	98 %	66	65
	21:50:39	0.06	110 %	98 %	66	65
	21:50:40	0.06	110 %	98 %	66	65

Participant three:

Measuring cycle	Time	R-value prototype	SpO2 prototype	SpO2 Sanitas	BPM Prototype	BPM Sanitas
	22:13:14	0,39	104 %	-	87	-
	22:13:19	0,16	108 %	-	86	-
	22:13:20	0,07	110 %	-	86	-
	22:13:21	0,31	106 %	-	86	-
1.	22:13:22	0,17	108 %	-	87	-
	22:13:23	0,16	108 %	-	86	-
	22:13:24	0,17	108 %	-	86	-
	22:13:25	0,2	108 %	-	87	-
	22:13:25	0,14	109 %	-	87	-
	22:13:26	0,12	109 %	-	88	-
	22:13:26	0,39	104 %	-	88	-
	22:13:27	0,19	108 %	-	89	-
	22:13:28	0,16	108 %	-	91	-
	22:13:28	0,07	110 %	-	93	-
2.	22:13:29	0,19	108 %	-	93	-
	22:13:30	0,25	107 %	-	93	-
	22:13:30	0,07	110 %	-	93	-
	22:13:31	0,08	110 %	-	92	-
	22:13:34	0,07	110 %	-	89	-
	22:13:36	0,23	107 %	-	89	-
	22:13:37	0,21	108 %	-	89	-
	22:13:37	0,23	107 %	-	89	-
	22:13:39	0,09	110 %	-	89	89
	22:13:39	0,31	106 %	97 %	96	89
3.	22:13:40	0,05	111 %	97 %	96	88
	22:13:41	0,22	107 %	97 %	96	87
	22:13:42	0,06	110 %	97 %	94	86
	22:13:43	0,05	111 %	97 %	93	86
	22:13:43	0,09	110 %	97 %	92	86
	22:13:44	0,07	110 %	97 %	91	85
	22:13:45	0,1	110 %	97 %	92	85
	22:13:46	0,04	111 %	97 %	82	84
	22:13:47	0,18	108 %	97 %	82	84
	22:13:48	0,16	108 %	97 %	82	84
4.	22:13:49	0,17	108 %	97 %	81	82
	22:13:49	0,16	108 %	97 %	81	82
	22:13:50	0,1	110 %	97 %	82	82
	22:13:51	0,12	109 %	97 %	83	82
	22:13:51	0,15	109 %	97 %	83	82
	22:13:52	0,01	111 %	97 %	82	83
	22:13:53	0,16	108 %	97 %	84	83
	22:13:54	0,22	107 %	97 %	85	83
	22:13:54	0,19	108 %	97 %	87	83
	22:13:55	0,05	111 %	97 %	88	84
5.	22:13:56	0,19	108 %	97 %	87	85
	22:13:56	0,04	111 %	97 %	87	85
	22:13:57	0,08	110 %	97 %	87	85
	22:13:58	0,14	109 %	97 %	86	86
	22:13:58	0,08	110 %	97 %	87	86
	22:13:59	0,04	111 %	98 %	87	86
	22:14:00	0,07	110 %	98 %	87	87
	22:14:01	0,12	109 %	98 %	87	87
	22:14:02	0,08	110 %	98 %	86	86
	22:14:02	0,1	110 %	98 %	87	86
6.	22:14:03	0,06	110 %	98 %	87	86
	22:14:04	0,06	110 %	98 %	87	86
	22:14:04	0,11	109 %	98 %	87	86
	22:14:05	0,07	110 %	98 %	86	85
	22:14:06	0,14	109 %	98 %	86	84
	22:14:06	0,04	111 %	98 %	86	84
	22:14:07	0,07	110 %	98 %	86	84
	22:14:08	0,09	110 %	98 %	86	84
	22:14:09	0,12	109 %	98 %	87	85
	22:14:09	0,12	109 %	98 %	87	85

7.	22:14:10	0,1	110 %	98 %	87	86
	22:14:11	0,04	111 %	98 %	87	87
	22:14:11	0,17	108 %	98 %	87	87
	22:14:12	0,07	110 %	98 %	88	87
	22:14:13	0,1	110 %	98 %	88	87
	22:14:15	0,1	110 %	97 %	88	88
	22:14:15	0,18	108 %	97 %	88	88
	22:14:17	0,22	107 %	97 %	91	88
	22:14:25	0,2	108 %	97 %	89	88
	22:14:26	0,19	108 %	97 %	90	88
8.	22:14:27	0,12	109 %	97 %	89	89
	22:14:28	0,15	109 %	97 %	89	89
	22:14:28	0,05	111 %	97 %	88	89
	22:14:29	0,08	110 %	97 %	88	89
	22:14:30	0,12	109 %	97 %	88	89
	22:14:30	0,18	108 %	97 %	88	89
	22:14:32	0,15	109 %	97 %	87	90
	22:14:40	0,1	110 %	97 %	88	91
	22:14:41	0,13	109 %	97 %	91	91
	22:14:41	0,11	109 %	97 %	89	91
9.	22:14:42	0,13	109 %	97 %	89	91
	22:14:42	0,11	109 %	97 %	89	91
	22:14:43	0,18	108 %	97 %	90	90
	22:14:44	0,3	106 %	97 %	90	90
	22:14:44	0,18	108 %	97 %	90	90
	22:14:45	0,05	111 %	97 %	90	90
	22:14:46	0,13	109 %	97 %	90	90
	22:14:47	0,16	108 %	97 %	90	90
	22:14:47	0,16	108 %	97 %	90	90
	22:14:48	0,06	110 %	97 %	90	90
10.	22:14:49	0,15	109 %	97 %	90	90
	22:14:50	0,27	106 %	97 %	90	90
	22:14:51	0,18	108 %	97 %	90	90
	22:14:51	0,36	105 %	97 %	90	90
	22:14:52	0,39	104 %	97 %	90	90
	22:14:53	0,11	109 %	97 %	90	91
	22:14:53	0,26	107 %	97 %	90	91
	22:14:55	0,27	106 %	97 %	90	90
	22:14:55	0,26	107 %	97 %	90	90
	22:14:57	0,09	110 %	97 %	92	90
11.	22:15:12	0,08	110 %	97 %	90	89
	22:15:13	0,1	110 %	97 %	89	89
	22:15:14	0,1	110 %	97 %	89	89
	22:15:14	0,17	108 %	97 %	88	89
	22:15:15	0,27	106 %	97 %	89	88
	22:15:16	0,34	105 %	97 %	88	88
	22:15:16	0,21	108 %	97 %	88	88
	22:15:17	0,11	109 %	97 %	88	88
	22:15:18	0,13	109 %	98 %	87	88
	22:15:18	0,09	110 %	97 %	87	88
12.	22:15:19	0,19	108 %	97 %	87	87
	22:15:20	0,31	106 %	97 %	87	87
	22:15:20	0,2	108 %	97 %	86	87
	22:15:21	0,26	107 %	97 %	86	88
	22:15:22	0,33	105 %	97 %	86	88
	22:15:22	0,37	104 %	97 %	87	88
	22:15:23	0,18	108 %	97 %	87	88
	22:15:24	0,12	109 %	97 %	87	88
	22:15:25	0,09	110 %	97 %	88	89
	22:15:25	0,22	107 %	97 %	88	89

13.	22:15:26	0,47	103 %	97 %	88	88
	22:15:26	0,16	108 %	97 %	90	88
	22:15:27	0,31	106 %	97 %	90	89
	22:15:31	0,43	103 %	97 %	90	89
	22:15:32	0,33	105 %	97 %	90	89
	22:15:32	0,15	109 %	97 %	90	89
	22:15:33	0,22	107 %	97 %	90	90
	22:15:34	0,31	106 %	97 %	90	90
	22:15:34	0,27	106 %	97 %	90	90
	22:15:35	0,33	105 %	97 %	90	90
14.	22:15:35	0,18	108 %	97 %	90	90
	22:15:37	0,19	108 %	97 %	89	91
	22:15:38	0,16	108 %	97 %	89	91
	22:15:39	0,28	106 %	97 %	89	90
	22:15:45	0,13	109 %	97 %	88	88
	22:15:45	0,34	105 %	97 %	86	88
	22:15:46	0,2	108 %	98 %	89	88
	22:15:47	0,29	106 %	98 %	89	89
	22:15:47	0,25	107 %	98 %	89	89
	22:15:48	0,19	108 %	98 %	89	89
15.	22:15:49	0,26	107 %	98 %	89	90
	22:15:50	0,17	108 %	98 %	89	89
	22:15:50	0,39	104 %	98 %	88	89
	22:15:51	0,34	105 %	98 %	88	88
	22:15:52	0,45	103 %	98 %	89	88
	22:15:53	0,2	108 %	98 %	88	88
	22:15:53	0,21	108 %	98 %	87	87
	22:15:54	0,31	106 %	98 %	87	87
	22:15:55	0,28	106 %	98 %	87	87
	22:15:55	0,23	107 %	98 %	87	87
16.	22:15:56	0,33	105 %	98 %	87	88
	22:15:57	0,25	107 %	98 %	87	88
	22:15:58	0,46	103 %	98 %	87	88
	22:15:59	0,55	101 %	98 %	86	88
	22:15:59	0,22	107 %	98 %	86	88
	22:16:00	0,28	106 %	98 %	87	88
	22:16:01	0,27	106 %	98 %	87	87

Eidesstaatliche Erklärung

Hiermit versichere ich eidesstaatlich, dass ich die vorliegende Arbeit selbstständig und ohne Benutzung anderer als der angegebenen Hilfsmittel angefertigt habe. Alle Stellen, die wörtlich oder sinngemäß aus veröffentlichten und nicht veröffentlichten Schriften entnommen sind, wurden als solche kenntlich gemacht.

Die Arbeit wurde in gleicher oder ähnlicher Form keinem anderen Prüfungsamt vorgelegt. Mir ist bewusst, dass eine falsche Erklärung rechtliche Folgen haben wird.

Bremen, 28.04.2022
Ort, Datum

Unterschrift